Radial Density Distribution of Negative Atomic Oxygen in the Oxygen Positive Column: An Experiment

THESIS

J. Mark DelGrande
Second Lieutenant, USAF

AFIT/GEP/ENP/86D-3

DEPARTMENT OF THE AIR FORCE
AIR UNIVERSITY
AIR FORCE INSTITUTE OF TECHNOLOGY

Wright-Patterson Air Force Base, Ohio

AFIT/GEP/ENP/86D-3

Radial Density Distribution of Negative Atomic Oxygen in the Oxygen Positive Column: An Experiment

THESIS

J. Mark DelGrande
Second Lieutenant, USAF

AFIT/GEP/ENP/86D-3

Approved for public release; distribution unlimited

AFIT/GEP/ENP/86D-3

RADIAL DENSITY DISTRIBUTION OF NEGATIVE ATOMIC OXYGEN IN THE OXYGEN POSITIVE COLUMN: AN EXPERIMENT

THESIS

Presented to the Faculty of the School of Engineering
of the Air Force Institute of Technology
Air University
In partial Fulfillment of the
Requirements for the Degree of
Master of Science in Engineering Physics

J. Mark DelGrande, B.S.
Second Lieutenant, USAF

December 1986

Preface

What you are about to read encompasses many of the areas of research which fall under the universal science known as physics. Over the past three months I have been both spectroscopist and plasma scientist, electrical engineer and theoretician, computor scientist and handyman. It is this aspect of physics that makes it the most rewarding and gratifying field of study.

It would not have been possible for me to have accomplished half of what I have were it not for the tremendous assistance I have received from the physics department at AFIT. Special thanks must go to Dr. Dorko with his help in my spectal measurements, Major Lupo with his computational and theoretical assistance, and of course Lt Colonel Evans, my advisor, who helped tremendously in the development of the new discharge design and construction.

Thanks must also be given to Dr. Alan Garscadden for helping me to understand the processes inside the oxygen positive column, and to Dr. Bish Gangully who helped in the development of the proposed optogalvonic experiment.

It has taken me many years to come this far. It seems only appropriate that I offer my greatest appreciation to the force that is my greatest inspiration. I dedicate this work to the memory of my mother: Cleta Mae.

J. Mark DelGrande

Contents

List of Figures

List of Symbols

α --dissociative attachment rate

β --ionization rate

c_s --ionic sound speed

γ --associative detachment rate

∂_i --partial derivative with respect to ith component

F_i --velocity average of the force on the ith species

h --ratio of negative ion density to electron density on axis

j,k --current densities

m --mass

n --species number density

q_i --ith component of species' average velocity

--(T_-/T_+) in Chapter 2.

σ --photodetachment cross-section in Chapter 5.

T_e --electron temperature (eV)

T_g --background gas temperature (eV)

$h\nu$ --energy per photon with frequency ν

f_a --accoustic wave frequency

ω_e --electron and ion plasma frequency

x_i --rectangular Cartesian coordinates

+, -, e : subscripts corresponding to positive ions, negative ions, and electrons respectively

Abstract

This thesis develops the foundation for an experiment to determine the radial distribution of the negative atomic oxygen ion in the positive column of a plasma discharge. Lee's theory (28) is modified to apply to a discharge of square cross-section. A new design for a discharge tube is presented. The operating characteristics of this tube are investigated: current-voltage measurements are made showing operating regimes of the T-form and H-form of the discharge, and accoustic waves are shown to exist in the T-form region. Three experimental designs are presented to determine the radial density of the oxygen anion, each involving photodetachment.

I. Introduction

Charged particles play an extensive role in the phenomena of the earth's upper atmosphere. For example, studies concerning the degradation of radar signals from the electron-ion densities in the atmosphere (41) require accurate modeling of charged particle interaction.

In 1924, Schottky (40) discussed the equilibrium of a cylindrical low pressure dc discharge plasma with two charged species: electrons and positive ions. Plasmas consisting of electronegative gases such as oxygen and iodine, however, contain high densities of negative ions. These negative ions cause an electronegative plasma to behave much differently than an electropositive gas such as argon. It seems only natural that Schottky's two body equilibrium theory be expanded to include the existence of negative ions.

Since oxygen is an atmospheric gas that is known to have lasing properties (28), it is a molecule of interest to plasma physicists. Because oxygen is an electronegative gas, a number of theories have been developed (10,22,27,33, 37,38,45) including the O^- ion as the third species in the oxygen positive column. In 1985, Clouse (8) showed that the best theory describing the three component plasma was the one developed by Lee.

Lee's theory is based on basic conservation equations, exchange rate assumptions, previously calculated mobility

and diffusion coefficients, as well as many other plasma interaction phenomena. While these assumptions are made to model a plasma in a gas discharge tube, they should also be applicable to other man-made plasmas in the lab as well as the plasma of the upper atmosphere.

It is the purpose of this paper to develop an experiment that will determine the distribution of negative ions in the positive column of an oxygen dc discharge. This paper will begin with a brief discussion of the fundamental principals of the dc dicharge, describing how a discharge operates, why we are interested in the positive column, and how such a discharge can be adapted for our experiment.

An adaption of Lee's theory to our experiment will follow. This should provide an understanding of the principal processes involved in the oxygen positive column of a gas discharge. We will then present a new design for the gas discharge which allows for quick, simple, and virtually limitless variation of the experimental apparatus. Such a design should prove useful not only for a follow-on experiment, but for numerous other discharge experiments where quick changes in design are desirable.

A discussion of the operating characteristics of our discharge will come next. Spectral observations will describe the various species in the discharge and in what way they are affected by changes in operating conditions. Voltage and current plots will be presented, and a theoretical presentation describing them will provide

further information as to what makes the oxygen column different from that of other gases. This will then lead to a discussion of acoustic wave phenomena which are characteristic of electronegative gas discharges. We will further discuss how these waves might affect our experiment and what can be done to minimize such an effect. We will then present some general difficulties that were encountered with our new chamber design and provide some ideas on how those difficulties might be solved.

Without time to obtain the proper equipment, the paper must conclude with three proposed experimental designs for determining the distribution of the O^- ion. These experiments include an absorption technique, and two variations of the optogalvanic technique. We will first discuss the theoretical thread that holds each of the three experiments together (photodetachment), and then provide a discussion and experimental set-up of each technique.

It is hoped this work will provide a firm foundation both theoretically and experimentally for a follow-on paper. Once the experimental data is collected, it can only provide greater insight into the validity of the assumptions made by Lee and others.

II. Fundamental Principles

Excellent discussion of the dc discharge and its many characteristics can be found in a number of references (7,23,46). A brief review is presented here so that the various regions of the glow discharge discussed in this paper can be identified and understood. Such a discharge operated at low pressure (1-10 Torr) and low currents (milliamps) is characterized by the many different regions shown in Figure 1.

Electrons leave the cathode passing through the Aston dark space. As they gain kinetic energy, electron multiplication through ionizing collisions takes place. Some of these collisions simply excite bound electrons to higher orbital states from which they radiate-- creating a region know as the cathode glow layer. Then in the cathode dark space the field becomes weaker and only a few highly energetic electrons interact. By the time the negative glow is reached, a large number of free electrons have been created. They have lost their ionization energy, but have enough energy to cause excitation.

It is in the negative glow that the number of electrons and ions becomes significant. Here, recombination begins to take place. With increasing distance from the cathode, fewer fast electrons are found, the probability of recombination decreases, less visible light is emitted and the Faraday dark space is created.

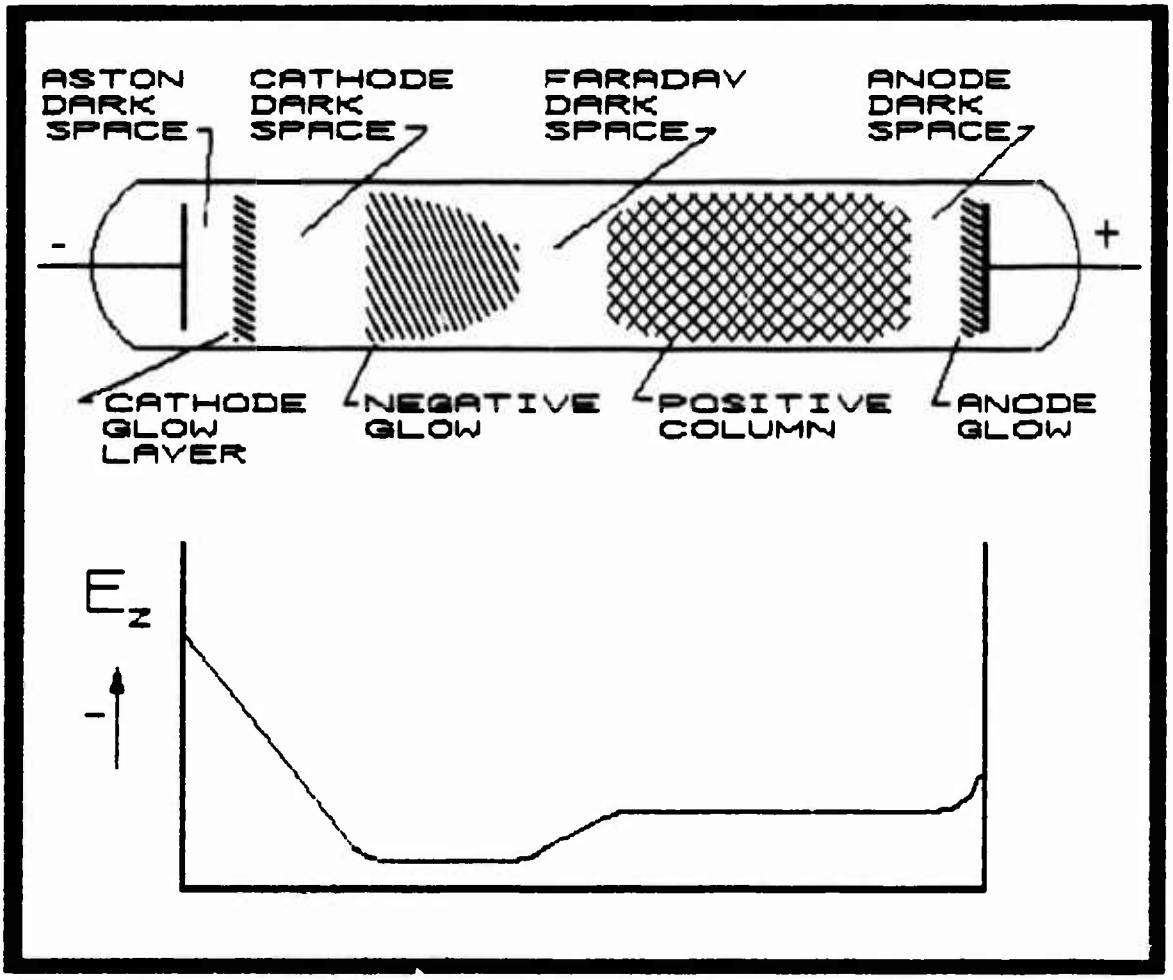

Fig 1. Regions of the Positive Column and Associated E-Field

Finally we reach the positive column--that part of the discharge which is most like a plasma. Here, positive and negative charge densities are almost equal, the axial electric field is constant at any point, and almost all ionizations are due to thermal interactions. The electrons, because of their greater mobility, carry almost all of the current on their way to the anode dark space. In the anode dark space the positive ions are repelled (negative space charge) and the small electron kinetic energy increases. The anode glow is created as the electrons gain sufficient kinetic energy to cause ionizations.

It is the positive column that is of interest to us, since it most resembles a plasma. We will therefore take a closer look at the theories of the positive column and adapt them to our experiment.

Oxygen Positive Column

In an oxygen discharge, the positive column is made up of electrons, positive ions and negative ions, in fact, the density of negative ions can sometimes outnumber the density of electrons by 10 to 1 (44:519).

There are a number of production and loss processes in an oxygen plasma. Rates, cross-sections, and energies of these reactions are given by Bacal (1) and Fehsenfeld (11). In the positive column, the production and loss of the various species reaches an equilibrium. The charged particles are produced and lost through collisional

interactions with each other and the discharge walls. These numerous processes lead to a variation of the densities of the charged species in the positive column. We wish to determine the negative ion densitiy distribution from the center of the discharge to the plasma's containment walls.

Lee models the equilibrium condition of the various plasma interactions by taking the appropriate moments of the Boltzman equation which lead to the conservation equations taking the form

$$(\partial n/\partial t) + [\partial(nq_k)/\partial x_k] = Q \tag{1}$$

$$(\partial q_i/\partial t) + q_k(\partial q_i/\partial x_k) = (F_i/m) - (\partial \sigma_{ik}/\partial x_k)/n + A \tag{2}$$

$$(3/2)(\partial T/\partial t) + (3/2)q_k(\partial T/\partial x_k) + T(\partial q_k/\partial x_k) = P - mA_k q_k + (Q/n)[(m/2)q_k q_k - (3/2)T] \tag{3}$$

The summation convention is invoked in these equations. Here x_i are rectangular Cartesian position coordinates, n is the given species' number density, m is its mass, q_i is the ith component of the species average velocity, F_i is the velocity average of the force experienced by a particle of the ith species, T is the species' kinetic temperature in energy units, and

$$Q \equiv \int_v (\partial f/\partial t) f(x,v,t) dv \tag{4}$$

represents production of the species by collisions.

The quantity σ_{ij} is defined by

$$\sigma_{ij} \equiv \int_v u_i u_j f(x,v,t)dv \qquad (5)$$

where $u = v - q$, and $f(x,v,t)$ is the species' single particle distribution function. The "drag" term A and the energy loss rate P for species produced in the operation of a discharge may be modeled by

$$A_i \equiv -\nu(q_i - q_i^{<0>}) \qquad (6)$$

and

$$P \equiv -\nu_0(T - T^{<0>}) \qquad (7)$$

where the subscript (0) refers to the background gas. These models introduce the species' momentum transfer frequency ν and energy transfer frequency ν_0.

According to Lee, the production and loss of the principal species in the oxygen discharge is best described by the reactions

$$O_2 + e^- \rightarrow O^- + O \qquad \text{(dissociative attachment)}$$
$$O^- + O \rightarrow O_2 + e^- \qquad \text{(associative detachment)}$$
$$O_2 + e^- \rightarrow O_2^+ + 2e^- \qquad \text{(ionization)}$$

Assuming a Maxwellian temperature distribution, Lee continues his model for a cylindrical discharge tube. The experimental techniques later proposed in this paper,

however, require that a laser be passed through the discharge tube in the transverse direction; the curved surface of a cylindrical glass tube creates many spurious reflections that are undesirable. It is then suggested that a tube with rectangular cross-section be constructed with the faces slightly offset to prevent multiple reflections.

To this end it was necessary to adapt Lee's theory to a cartesian system that would model such a square discharge.

Square Discharge Model

Following Lee's development, only for Cartesian symmetry, the particle conservation equations become

$$\partial_x k_e + \partial_y j_e = (\beta-\alpha) n_e + \gamma n_- \tag{8}$$

$$\partial_x k_- + \partial_y j_- = \alpha n_e - \gamma n_- \tag{9}$$

$$k_e(m_+\nu_+ + m_e\nu_e) + k_-(m_+\nu_+ + m_-\nu_-) = -(T_e+T_o)\partial_x n_e - 2T_o\partial_x n_- \tag{10}$$

$$j_e(m_+\nu_+ + m_e\nu_e) + j_-(m_+\nu_+ + m_-\nu_-) = -(T_e+T_o)\partial_y n_e - 2T_o\partial_y n_- \tag{11}$$

$$T_e n_- \partial_x n_e + m_e\nu_e n_- k_e = T_o n_e \partial_x n_- + m_-\nu_- n_e k_- \tag{12}$$

$$T_e n_- \partial_y n_e + m_e\nu_e n_- j_e = T_o n_e \partial_y n_- + m_-\nu_- n_e j_- \tag{13}$$

with boundary conditions

$$j_e(x,0) = j_-(x,0) = 0 \tag{14}$$

$$k_e(0,y) = k_-(0,y) = 0 \tag{15}$$

$$n_e(x,D) = n_-(x,D) = 0 \tag{16}$$

$$n_e(D,y) = n_-(D,y) = 0 \tag{17}$$

$$j_-(x,D) = k_-(D,y) = 0 \tag{18}$$

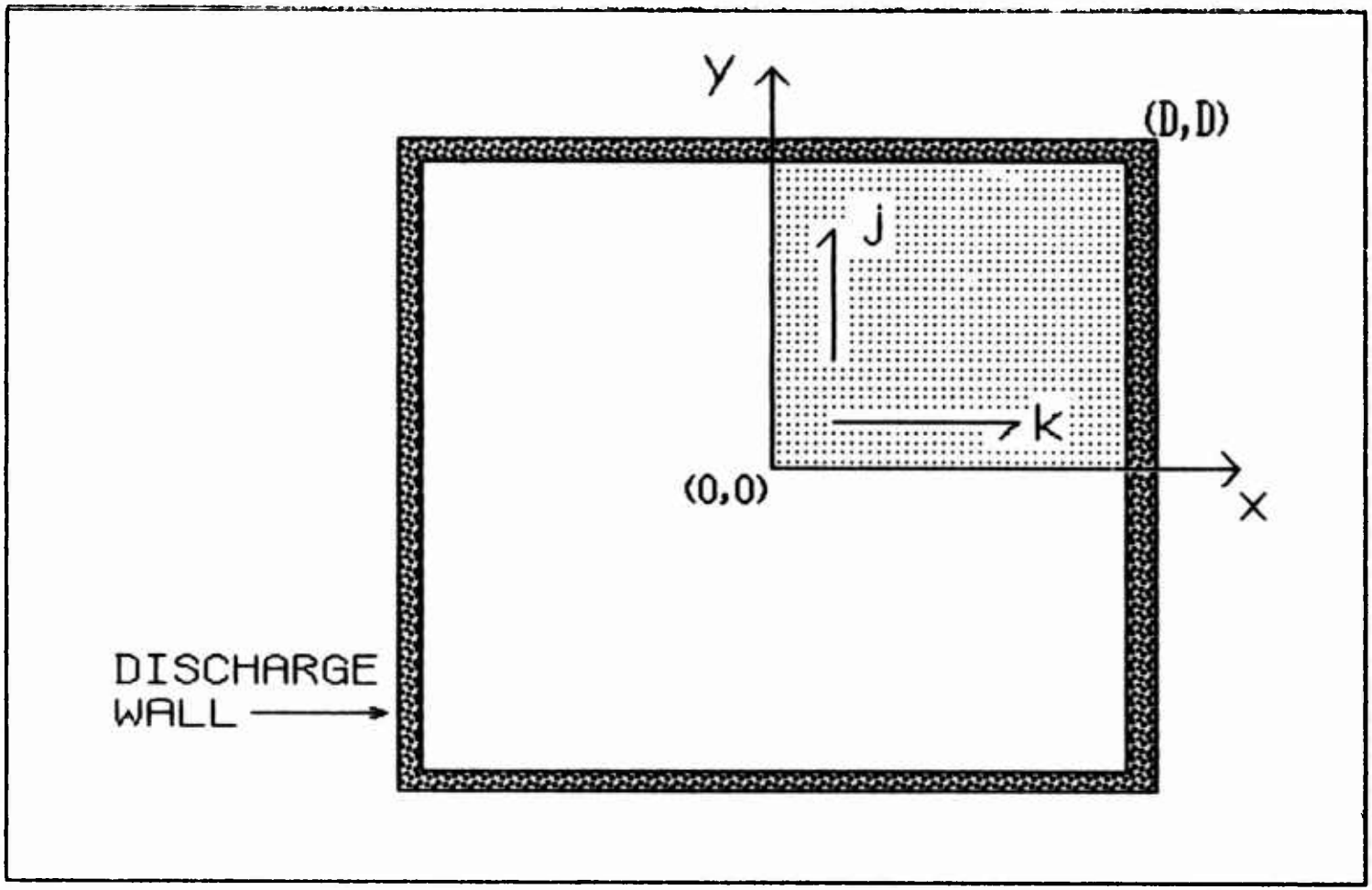

Fig 2. Current Vectors for a Square Discharge Tube

where

∂_i = partial derivitive with respect to ith component
α = dissociative attachment rate (s^{-1})
β = ionization rate (s^{-1})
γ = associative detachment rate (s^{-1})
T_e = electron Temperature (eV)
T_0 = background gas temperature (eV)
k_i = current density ($cm^{-2}s^{-3}$) for species i (where the subscript +, -, and e represent O_2^+, O^- and e^- respectively) in the x direction [See Figure 2.]
j_i = current density for species i in the y direction
D = distance to wall

The following nondimensionalization is convenient: let

$$p=x/D \tag{19a}$$

and

$$q=y/D \tag{19b}$$

and let

$$z_1(p,q)=n_e(x,y)/n_e(0,0) \tag{20a}$$

$$z_2(p,q)=n_-(x,y)/n_e(0,0) \tag{20b}$$

$$z_3(p,q)=j_e(x,y)/[\alpha n_e(0,0)D] \tag{21}$$

$$z_4(p,q)=j_-(x,y)/[\alpha n_e(0,0)D] \tag{22}$$

$$z_5(p,q)=k_e(x,y)/[\alpha n_e(0,0)D] \tag{23}$$

$$z_6(p,q)=k_e(x,y)/[\alpha n_e(0,0)D] \tag{24}$$

A two point boundary value problem is then developed when the proper substitutions are made which provides us with the following set of equations:

$$\delta_x z_5 + \delta_y z_3 = [(\beta-\alpha)/\alpha] z_1 + (\gamma/\alpha) z \tag{25}$$

$$\delta_x z_6 + \delta_y z_4 = z_1 - (\gamma/\alpha) z_2 \tag{26}$$

$$\delta_x z_1 + 2\sigma\delta_x z_2 = -A z_5 - B z_6 \tag{27}$$

$$\delta_y z_1 + 2\sigma\delta_y z_2 = -A z_3 - B z_4 \tag{28}$$

$$z_2\delta_x z_1 - \sigma z_1\delta_x z_2 = (B-A) z_1 z_6 - C z_2 z_5 \tag{29}$$

$$z_2\delta_y z_1 - \sigma z_1\delta_y z_2 = (B-A) z_1 z_4 - C z_2 z_3 \tag{30}$$

with boundary conditions

$$z_1(0,0) = 1 \tag{31}$$

$$z_1(x,1) = z_1(1,y) = z_2(x,1) = z_2(1,y) = 0 \tag{32}$$

$$z_3(x,0) = z_4(x,0) = 0 \tag{33}$$

$$z_5(0,y) = z_6(0,y) = 0 \tag{34}$$

where

$$\sigma = (T_o/T_e)$$
$$A = [m_+ \upsilon_t \alpha D^2]/T_e$$
$$B = A + [m_- \upsilon_- \alpha D^2]/T_e$$
$$C = [m_e \upsilon_e \alpha D^2]/T_e$$

If we represent the ratio of the negative ion number density to electron number density at the discharge axis as

$$h \equiv n_-(0,0)/n_e(0,0) \tag{35}$$

and let

$$z_2 \equiv h z_1 \tag{36}$$

then, following Lee, equations (25)--(30) lead to

$$\delta_x z_5 + \delta_y z_3 = [(\beta-\alpha)/\alpha + (\gamma/\alpha)] z_1 \quad (37)$$

$$\delta_x z_6 + \delta_y z_4 = [1-(\gamma/\alpha)h] z_1 \quad (38)$$

$$(1+2\sigma h)\delta_x z_1 = -Az_5 - Bz_6 \quad (39)$$

$$(1+2\sigma h)\delta_y z_1 = -Az_3 - Bz_4 \quad (40)$$

$$h(1-\sigma)\delta_x z_1 = (B-A)z_6 - Chz_5 \quad (41)$$

$$h(1-\sigma)\delta_y z_1 = (B-A)z_4 - Chz_3 \quad (42)$$

We can now solve for z_4, z_6, z_3, and z_5 in terms of z_1 using equations (39)--(42). This gives us

$$z_4 = h\{[-C(1+2\sigma h)+A(1-\sigma)]/[A(B-A)+BCh]\}\delta_y z_1 \quad (43)$$

$$z_6 = h\{[-C(1+2\sigma h)+A(1-\sigma)]/[A(B-A)+BCh]\}\delta_x z_1 \quad (44)$$

$$z_3 = -\{[(B-A)(1+2\sigma h) + Bh(1-\sigma)]/[A(B-A) + BCh]\}\delta_y z_1 \quad (45)$$

$$z_5 = -\{[(B-A)(1+2\sigma h) + Bh(1-\sigma)]/[A(B-A) + BCh]\}\delta_x z_1 \quad (46)$$

Substituting these into equations (37) and (38) we have

$$-\{[(B-A)(1+2\sigma h)+Bh(1-\sigma)]/[A(B-A)+BCh]\}\delta_{xx} z_1$$
$$-\{[(B-A)(1+2\sigma h)+Bh(1-\sigma)]/[A(B-A)+BCh]\}\delta_{yy} z_1$$
$$= [(\beta-\alpha)/\alpha + (\gamma/\alpha)h] z_1 \quad (47)$$

and

$$h\{[A(1-\sigma)-C(1+2\sigma h)]/[A(B-A)+BCh]\}\delta_{xx} z_1$$
$$+ h\{[A(1-\sigma)-C(1+2\sigma h)]/[A(B-A)+BCh]\}\delta_{yy} z_1$$
$$= [1-(\gamma/\alpha)h\ z_1 \quad (48)$$

If we set

$$(S_1)^2 = \{[A(B-A)+BCh]/[(1+2\sigma h)(B-A)+Bh(1-\sigma)\} * [(\beta-\alpha)/\alpha + (\delta/\alpha)h] \quad (49)$$

and

$$(S_1)^2 = (1/h)\{[A(B-A)+BCh]/[A(1-\sigma)-C(1+2\sigma h)]\} * [h(\gamma/\alpha) - 1] \quad (50)$$

we reduce equations (47) and (48) to the simple boundary value equation

$$\delta_{xx}z_1 + \delta_{yy}z_1 = -(S_1)^2 \quad (51)$$

which gives us

$$z_1(p,q) = \cos[(S_1/2^{1/2})p]\cos[(S_1/2^{1/2})q] \quad (52)$$

and

$$z_2(p,q) = h\{\cos[(S_1/2^{1/2})p]\cos[(S_1/2^{1/2})q]\} \quad (53)$$

where

$$S_1 = 2(\pi/2)^2]^{(1/2)} = 2.2214... \quad (54)$$

which compares to Lee's value for $S_1 = 2.4048....$

The coefficients of Lee's Sylvester determinant (27:4702) did not vary significantly with such a small change in S_1. This allowed us to use the same solutions for T_e and h obtained by Lee (Fig. 3 and 4).

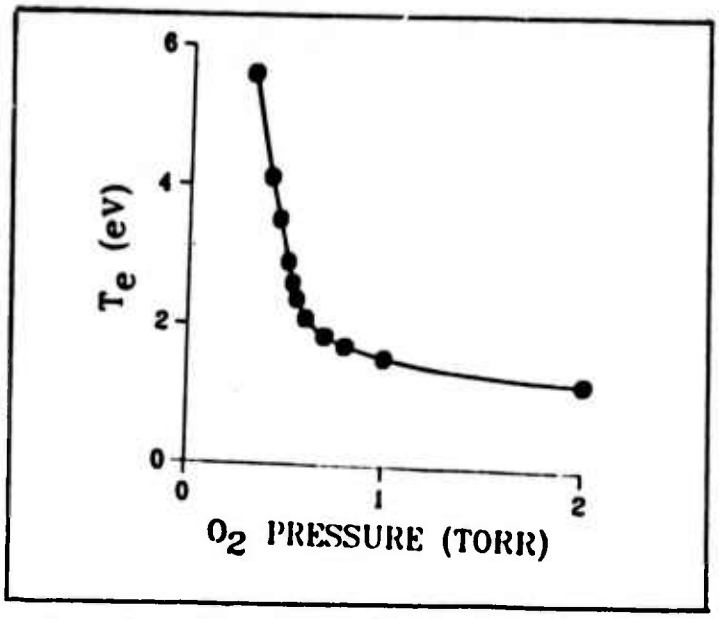

Fig 3. Electron Temperature vs. Pressure (Adapted from Lee:27)

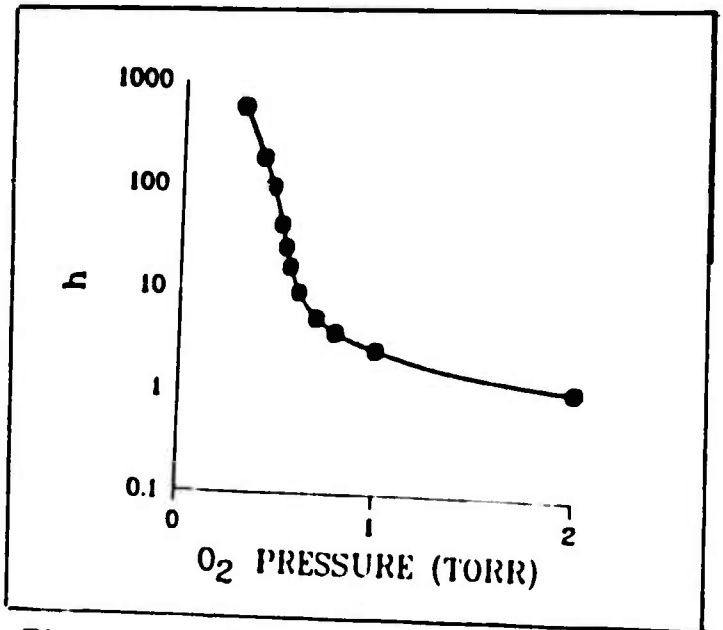

Fig 4. Ion to Electron Density Ratio vs. Pressure (Adapted from Lee:27)

The equation for z_2 can now be put into a simple square matrix, the rows of which are integrated to give the density distribution as seen by a laser scanning in the transverse direction of a square discharge from its center to the wall. Figure 5 shows the normalized distribution of such a scan.

Attempts were made to obtain numerical solutions to the differential equations using finite differencing. This method proved unsuccessful due to the large dynamic range of the problem. Densities change from zero to 10^{12} too rapidly for a stepwise convergence. Lee references Shampine (42) for the code he used in obtaining numerical solutions. Further effort in this direction might prove informative, but the analytic solution given above should provide an adequate reference for comparison against experiment.

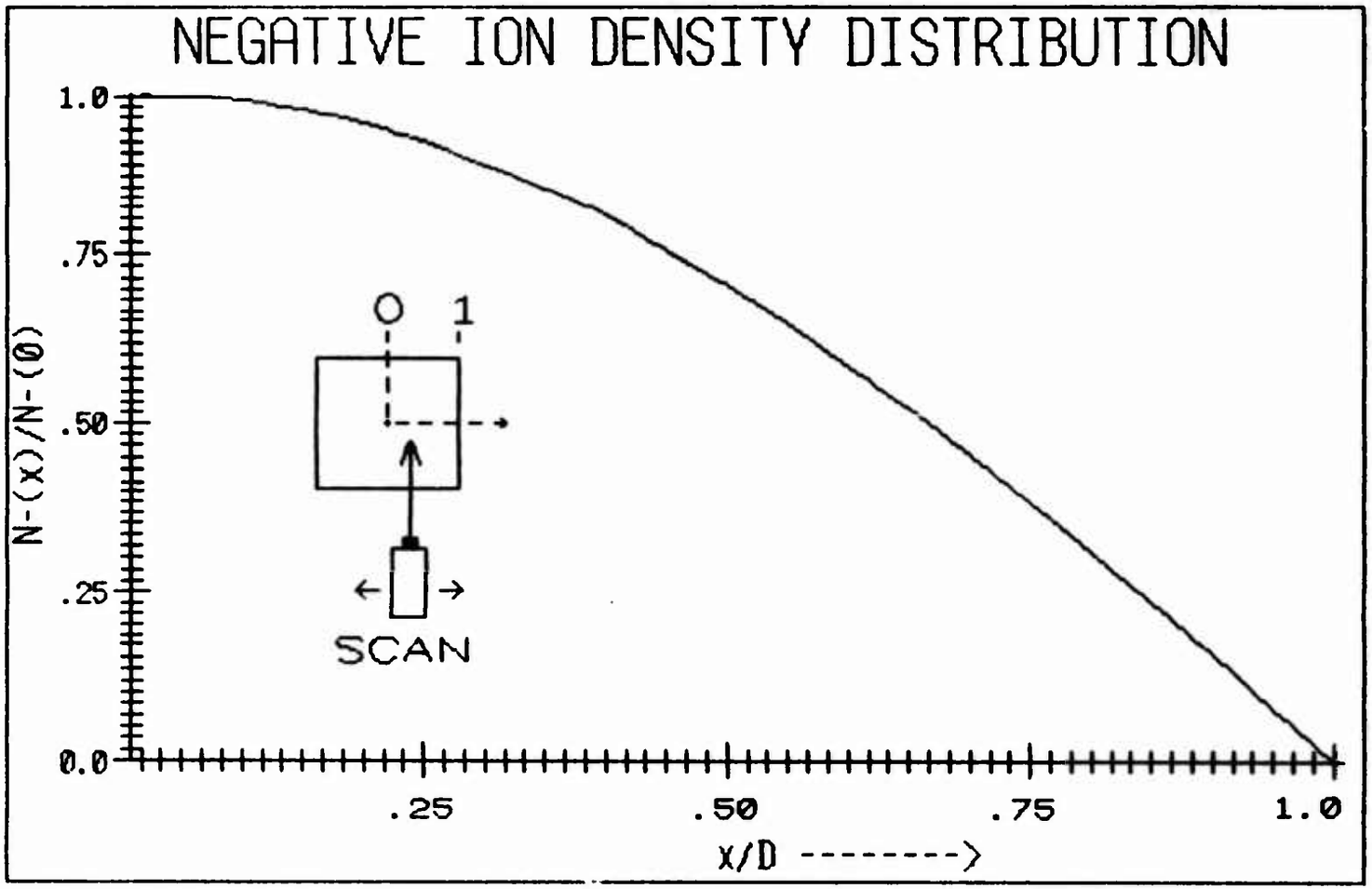

Fig 5. Negative Atomic Oxygen Ion Density Distribution as seen by a Laser Scanning from 0 to 1.

III. Experimental Design

A significant amount of time went into the design and construction of the experimental apparatus. Many obstacles had to be overcome to obtain a dc discharge that could be quickly adapted to conform to a variety of experimental tests. We have developed a discharge chamber that can perform all three of the experiments presented in this thesis to determine the density of the O^- ion.

We present in this chapter the design of the experimental apparatus. We will discuss some of the difficulties that arose in its construction, and make some suggestions that will improve upon the design in further experiments.

Design of the Discharge Chamber

The main vacuum chamber (Figure 6) consisted of a six way cross seven inches in length, a four way cross seven inches in length and three plexiglass inserts three inches in length. These pieces were held together with quick-connects and sealed with standard o-rings.

A five centimeter inside diameter glass tube, which contains the discharge, fit inside this chamber, supported by plexiglass cradles. Adjustable electrodes slid in from either side of the glass tube and allowed for variation in discharge length from 10 to 45 cm. They were held to the main chamber with plexiglass caps. Four plexiglass viewports located at the chamber crosses made viewing of both cathode and anode possible. They also permitted laser

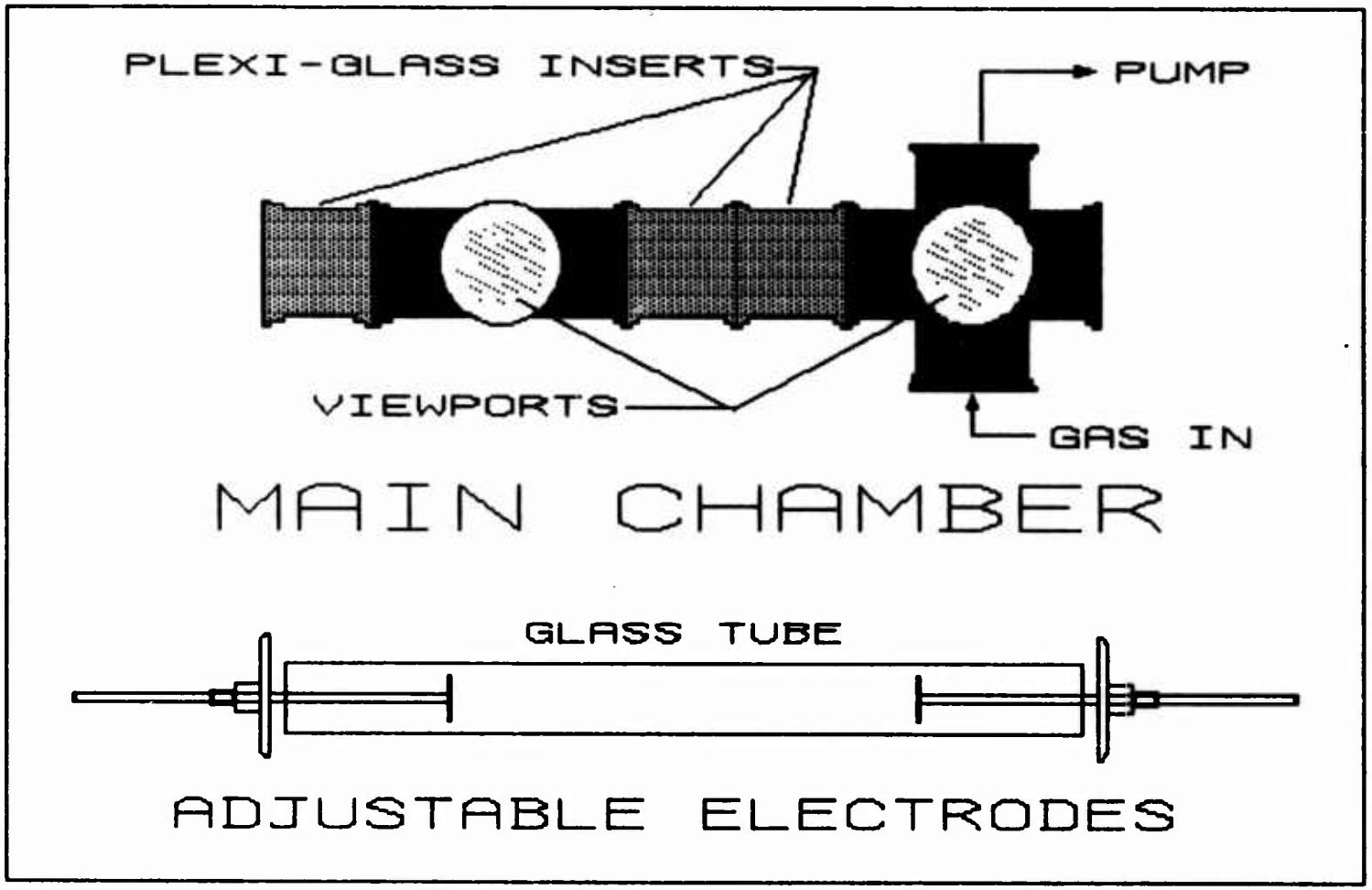

Fig 6. Discharge Main Chamber

light to be passed through the positive column of the discharge.

While the plexiglass inserts do allow for better viewing of the overall discharge, their major purpose was to prevent arcing to the tube walls. When metal inserts were used in the chamber, we found that by separating the electrodes more than about 20cm they would discharge to the metal chamber walls. This path afforded the least resistance to the electric current. In order to increase that resistance, the plexiglass inserts were used. Another insert was used to insulate the main chamber from the rest of the vacuum system, including the pumps and pressure guages. The three plexiglass inserts allowed for a discharge length of up to 45cm without arcing. If a longer discharge is desired, a greater number of inserts must be used.

Electrical Design

The overall electrical circuitry of the discharge is shown in Figure 7. The cathode was maintained at ground potential while a positive voltage was applied to the anode side. The power supply was capable of 10kV and 400mA of dc power. The discharge, however, was never run above 100mA to prevent overheating.

The electrodes were constructed of aluminum disks, 3.8cm diameter, connected to aluminum rods. They were broken in by a gradual increase in discharge current to slowly create an even oxidation of the surfaces. The electrodes were cleaned after about twenty hours of use.

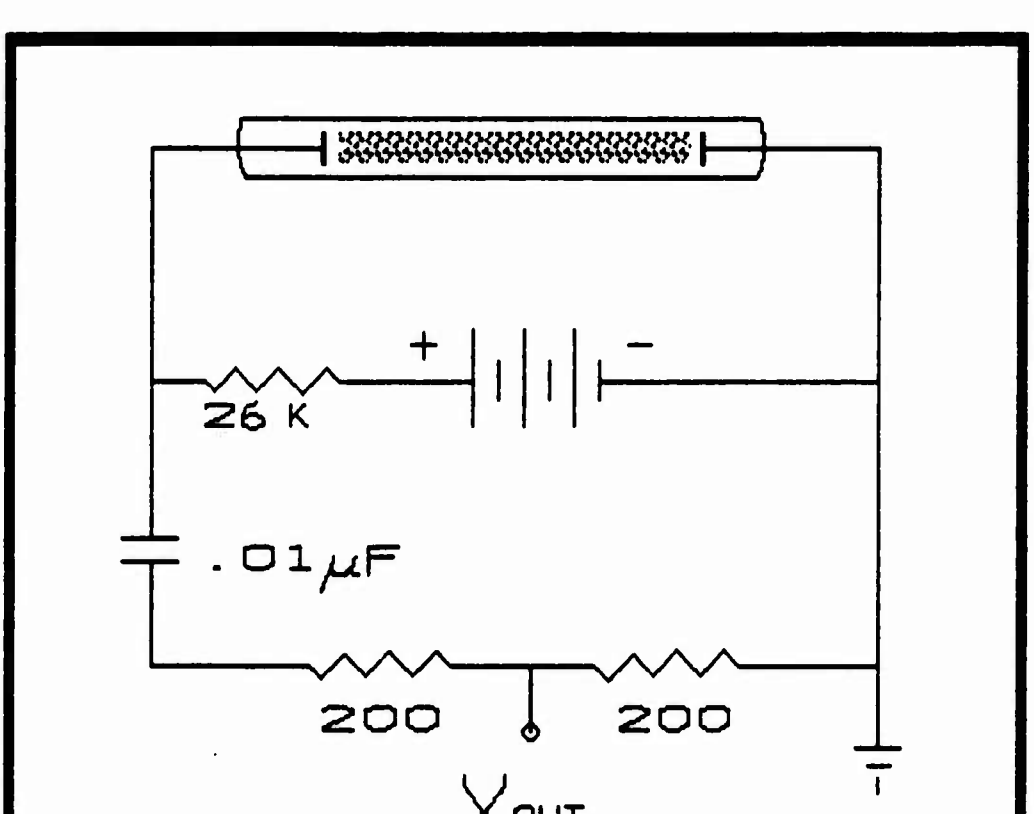

Fig 7. Electrical Design Scematic

Gas System

The system was evacuated with two roughing oil pumps capable of lowering the pressure to .01 Torr with no flow. They readily provided flow pressures from .5 to 10 Torr (our region of interest). Pressure stability, however, was not satisfactory since the pumps tended to cycle. This proved to be a small problem later in observing the various acoustic waves. Still, pressures were maintained to within $\approx$.1 Torr.

Since argon has been used so extensively in discharges in the past, it was used to test the system after initial construction. Using argon, we first observed arcing to the chamber walls and other problems. Once these difficulties were eliminated, ultra-high purity oxygen was used for the discharge experiments.

The gas was bled into the system directly through the bottom of the main chamber. Pressure was maintained with a needle valve and monitored with a Baritron guage at the top of the main chamber. A further guage measured the pressure at the pumps some six feet from the main chamber. Although not passing through the glass discharge tube directly, a positive flow was maintained at all times. This decreased the buildup of contaminants in the discharge tube. The system's throughput was less than 10 torr liter/sec.

Difficulties and Improvements

The present system is placed upon a wood foundation. Since the pumps run continuously in this experiment, there

is extraneous vibration of the main chamber. This becomes a problem when spectroscopic measurements are performed, or if a precise region of the discharge is to be irradiated with a laser. In order to minimize this problem, it is suggested that a floating table be used to support the main chamber.

The pumps also have a tendency to cycle. That is, they don't pump at a steady rate, but tend to increase and decrease the flow rate in a periodic manner. This becomes a problem in pressure stability as well as vibration, and is particularly noticeable as an irregularity in observing acoustic waves. This should not prove to be too much of a difficulty in the experiments presented here, but it is a problem that should be noted. In general, the overall gas system could be improved with better pumps, more accurate and readable guages and more precise pressure adjustment.

There is another observation that is not of major concern but is worth noting. Both the aluminum disc and rod act as an electrode in the discharge. This is particularly noticeable in the cathode glow. As the current is increased or the pressure is decreased, the cathode glow tends to envelop the disc and then glow around the rod. Increasing the current further causes the glow to cover more of the rod. This could make it difficult to determine how much area of the electrode is actually being used by the discharge. If this is of concern, then the rod should be coated with an insulating material.

It was also noted that as the glow on the cathode grew, the electrode became warmer. The temperature became so hot

that it caused the plexiglass cap holding the electrode to warp. This could be a significant problem if the discharge is run at high currents (greater than 50 mA) for long periods of time (over an hour). Some sort of cooling device (perhaps a fan) should be used if it is necessary to run the discharge in these conditions.

The experiments presented in this thesis should not require any major modification of the present discharge design. The precautions listed above may, however, prove useful if another experiment is performed using this chamber.

IV. Experimental Observations

Various diagnostics were performed on the oxygen discharge to determine if some of its characteristics might affect our proposed experiments to determine the negative ion density. We were primarily concerned with how pure the oxygen discharge was and how similar its electronic characteristics were to experiments performed in the past.

We will first discuss the species that were spectroscopically observed in the discharge; it is shown that the densities of certain species in the discharge vary as the operating conditions are changed. We will then discuss the voltage vs. current characteristics of the discharge. We will further discuss why the voltage-current relationship should behave as it does at various pressures. We will then present a discussion of the observed strata in the discharge. Finally, we will show why it is believed that these strata are acoustic waves. Throughout this chapter we will examine what role these charactistics might have on our proposed experimental designs.

While our new chamber design facilitates the discharge's adaptability to various experiments, we will show in this chapter that the observed phenomena are typical of discharge experiments in the past. It should further be noted that the experiments mentioned briefly in this chapter will be explained in detail in the following chapter. They are mentioned here to help explain observed phenomena.

Spectroscopic Experiment

At around 4 Torr and 25 mA, the positive column of the oxygen discharge appears as a grey-violet glow that is somewhat constricted within the glass tube. As the pressure is decreased and the current increased, the glow begins to fill the tube and becomes a much more intense grey-pink.

The tube was monitored through a viewport positioned at the positive column. The emitted light was passed through a f/3.5 lens and focussed on a .3 meter, f/5.3, McPherson monochrometer (see Figure 8). An f/5.3 lens, which would have matched light gathering power to the monochrometer was not available. With 10μm slits the resolution of the system is .06nm. The signal was monitered by an RCA C31034 photomultiplier and passed to a storage scope which in turn sent the desired wavelength scan to an X-Y plotter.

Scans were made from 350nm to 900nm (the limits of operation for the system). A number of atomic line and molecular band spectra were observed. It is beyond the scope of this paper to present in detail the transitions of each of the observed spectral lines. We will simply discuss the observed species and how they may or may not affect our proposed experiments.

Lee identifies the major species in the oxygen discharge as O_2, O, O_2^+, and O^-. Lewis (28) also notes the presence of O^+ and O_2^-. Of these species, only O, O_2^+, and O^+ were readily identified. With 800μm slits, the $b^1\Sigma_g^+$ transition (19:560) of O_2 ($\approx$760nm) was the only O_2 band observed.

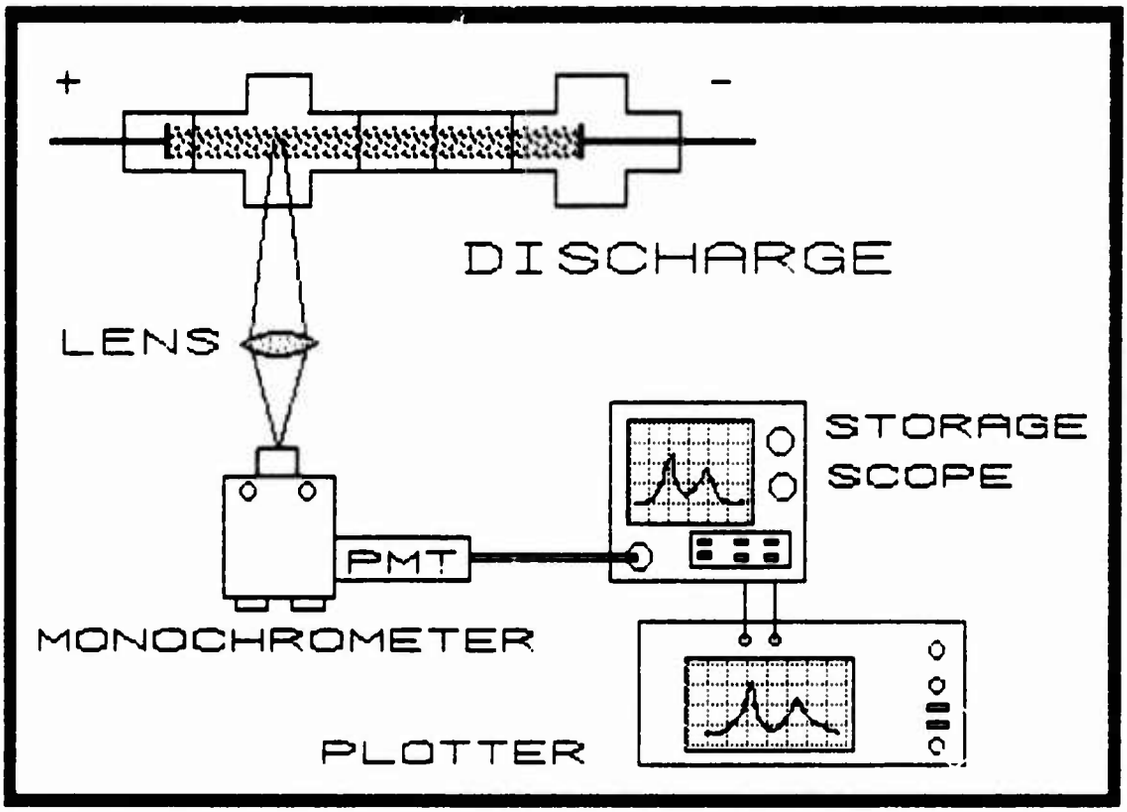

Fig 3. Spectroscopic Experimental Design

The most intense oxygen lines observed were the six $2p^3 3s$--$2p^3(^4S^o)3p$ lines of atomic oxygen--three near 777nm and three near 845nm.

Impurities were also observed. The 2s-3p transitions of hydrogen at 656nm and 486nm were easily observed (47:E-238), the 656nm being the most intense. It is believed that the hydrogen impurities are due to water vapor in the discharge. Before the experiment was run, the system was evacuated for only an hour. Some outgassing may have still been taking place. The evacuation of the system overnight should help to eliminate the hydrogen impurities.

Hydrogen was not the only impurity in the discharge system. Carbon monoxide (CO) bands were fairly intense throughout much of the spectrum. According to Pearse (32:115), the bands appear strongly in the positive column of a discharge with a mere trace of CO. Further, the glass of a new discharge tube contains sufficient amounts of CO to provide strong bands in both the Angstom and Third Positive system. To reduce the presence of the CO bands, there must be a sufficient break in period for the glass tube being used. It should be noted, however, that the CO bands do not come into play in any of the experiments that will be proposed in the following chapters.

There are a number of regions in the spectrum that could be of interest to us (see Chapter 5). At 632.8nm, no strong lines are observed. This suggests that a HeNe laser could be used in an absorption experiment. A doubled Nd:YAG laser

emits at 530nm. Such a laser could provide sufficient energy densities for an optogalvanic experiment. There are no strong lines from the discharge near 530nm. An argon-ion laser emits at 488nm and 514nm, which suggests that something must be done about the hydrogen impurity at 486nm, while the 514nm line has only the tail of a weak CO band near it. This laser might also be used for an optogalvanic experiment.

Voltage and Current Characteristics

When performing the spectroscopic runs, various parameters of the discharge were changed in order to obtain the brightest discharge. The parameters changed were voltage, current, pressure and tube length. The monochrometer was set to the bright OI line at 777nm and a 20 second scope trace showed variations in the OI intensity as the discharge parameters were changed within that time. Further note was taken of the visible changes taking place in the discharge.

At 1 Torr pressure, it was noted that as the current increased there was a sudden substantial brightening of the tube near 30 mA. The intensity of the OI line also increased. In an oxygen discharge, this is known as the transition from the T-form (or low field form) to the H-form (or high field form). Sabadil (39) characterizes the H-form of the discharge as being more highly dissociated than the T-form. He further states that in the H-form the atomic

line spectrum predominates, which would agree with our observation of a brightening of the OI line.

To see if we could increase brightness further, the discharge was set in the high field form at 1 Torr and 40 mA, and the tube length was varied from 25 cm to 40 cm. Since the discharge was extinguished each time the electrodes were moved, it was difficult to discern any visible change in the discharge (except for the obvious lengthening of the positive column). There was, however, a slight increase in intensity of the OI line observed on the scope. This agrees well with Rundle (36:3007) who shows that the atomic oxygen density increases linearly with increasing tube length.

At low currents (≈20 mA), lowering the pressure from 5 Torr caused the tube to suddenly brighten, which would suggest that the transition from T to H-forms is lowered at lower pressures. Voltage vs current plots (Figures 9 and 10) show this same result. Here, supply voltage vs. current was recorded at various pressures and tube lengths.

The general upward slope of these curves denotes the V=IR characteristic of the ballast resistor and the impedence of the total discharge (electrode to electrode). In actuality, the electric field of the positive column alone decreases slightly with increasing current as is seen by the similar, but much more precise curves, in Dettmer's dissertation (9:38). The slight decrease in electric field

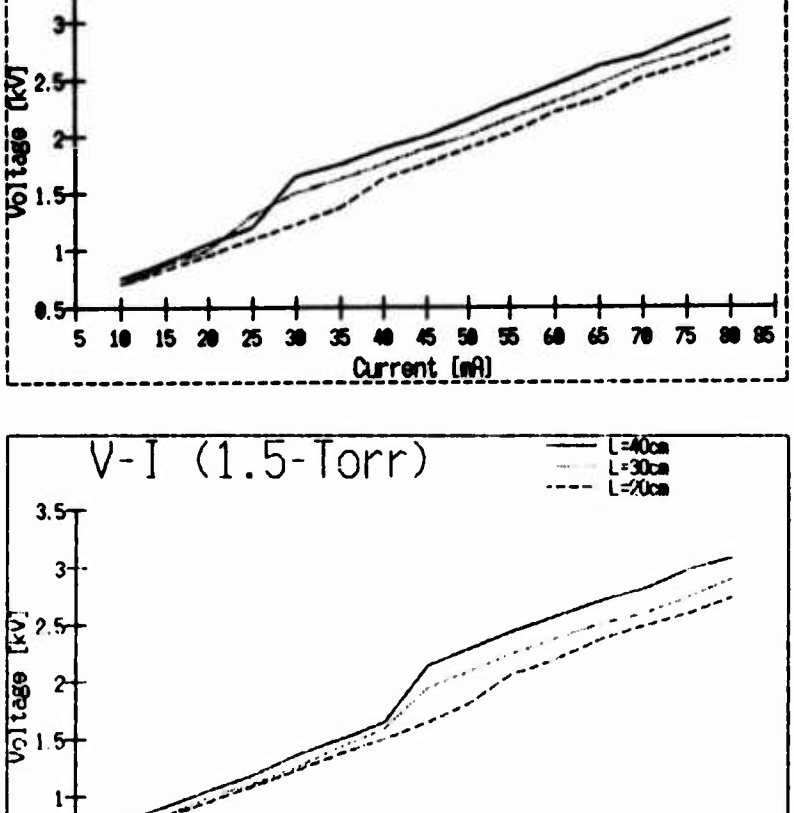

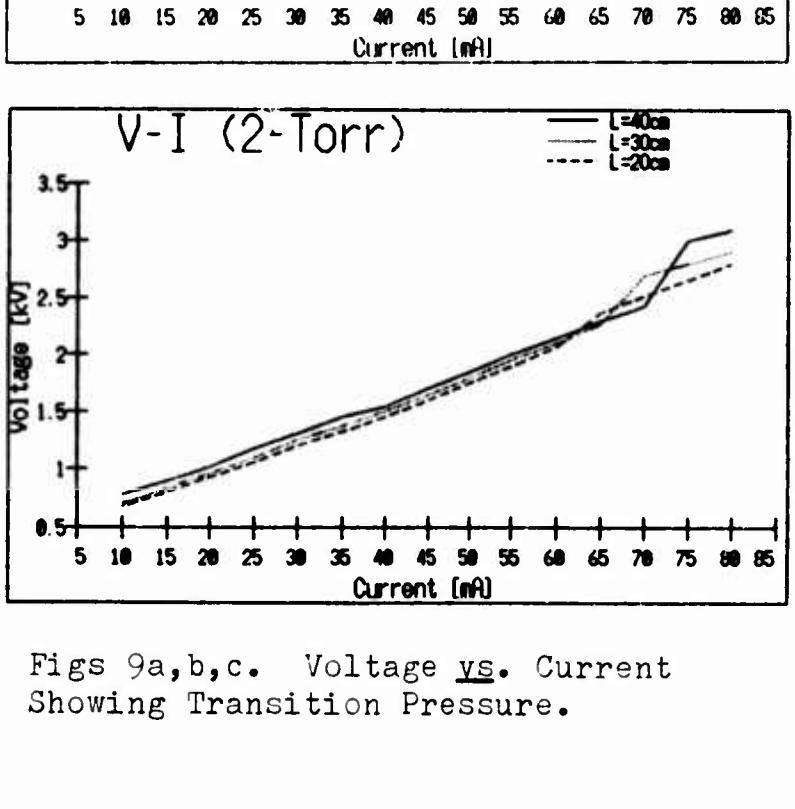

Figs 9a,b,c. Voltage vs. Current Showing Transition Pressure.

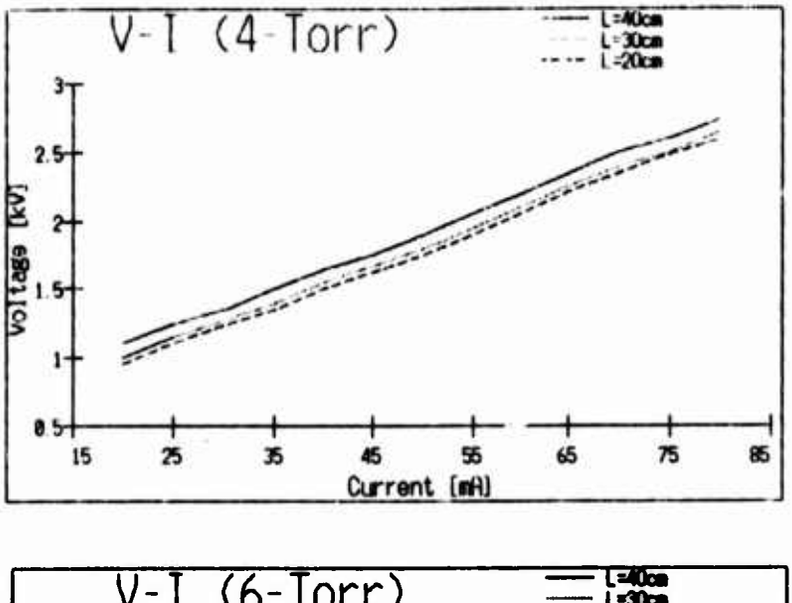

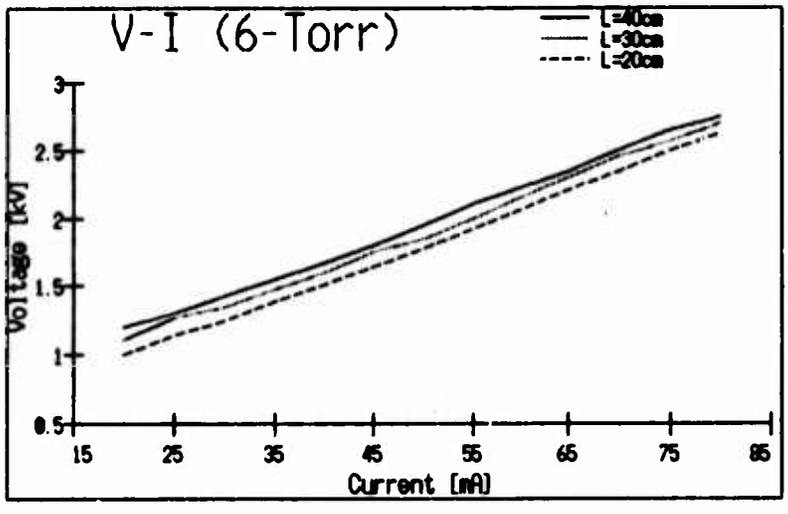

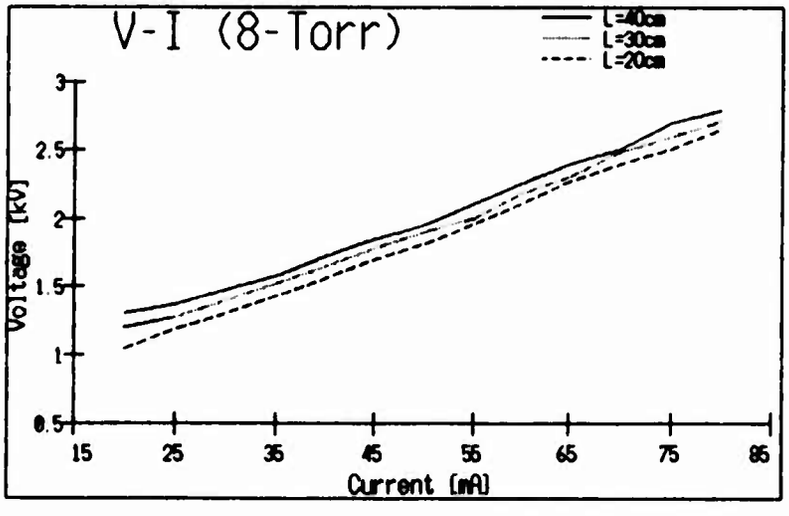

Figs 10a,b,c. Voltage vs. Current Above Transition Pressure

with current in the positive column is described by Ingold (23:47) as being due to the presence of two-step ionization.

The high field form of the oxygen discharge behaves much like an electro-positive discharge. The column is essentially a two-component plasma (electrons and positive ions) since the electron density dominates the negative ion density. Here, the attachment/detachment processes of the plasma are insignificant compared to direct molecular ionization. This is easily seen by comparing the reaction cross-sections to the electron energy distribution function of Dettmer (9:135,240-253).

If we lower the reduced electric field strength (E/N), however, the ionization cross-section decreases. At transition, the ionization process decreases rapidly, while attachment/detachment processes suddenly dominate. It is observed that the negative ion density begins to dominate the electron density. The column becomes a three-component plasma.

Since the attachment/detachment processes merely transfer electrons back and forth, any true losses must be balanced by ionization if the discharge is to sustain itself. The discharge accomplishes this by adjusting itself to enhance ionization (increasing E/N) and then relaxing to the attachment/detachment processes. In essence, the reduced field in the discharge oscillates back and forth between ionization and attachment/detachment processes. The net effect of these oscillations is a lowering of the

overall field and the creation of accoustic waves--the discharge has entered the low field form.

Figures 9 and 10, show the sudden increase in the discharge voltage at the transition region. They also show, as do Dettmer's plots, that the transition region occurs at higher currents for higher pressures. An increase in the pressure decreases the reduced field strength (E/N). Thus, the low field form of the discharge is enhanced and higher currents are required to achieve transition from the low to high field forms.

There are a number of other phenomena that occur within the discharge in its various forms. The above discussion is but a small part of the overall picture that causes the discharge to transition from the low to high field form. If one is to model fully the transition process, such things as ionization cross-sections of various metastable states, variations in electron distibuton and temperature, radial variations of densities and distribution functions as well as many others, must all be taken into account. Various approximations to these factors are listed by Franklin (12:37).

Acoustic Waves

The instabilty of the T-form of the oxygen discharge can be characterized by the existence of oscillations (or strata) in the electric field of the discharge. Sabadil interprets the strata of the oxygen discharge, which are

significantly different from the strata seen in other gas discharges, as ionic sound waves (39).

It was shown above that the T-form exists at low currents. As the current is increased past transition, the stable, homogenous H-form is achieved. This region has no observable oscillations or strata. It should be noted that at very low currents (≈1 mA) and pressures greater than about 1 Torr, a high field or H-form with strata is reported to exist by Sabadil. We were unable to examine this region since the discharge could not be maintained below 15 mA.

The discharge's oscillatory behavior was investigated at pressures from .5 to 3 Torr, and currents from 20 to 80 mA. A 0.01μF capacitor was connected to the anode side of the discharge. In order to reduce the signal a simple low impedance voltage divider was used. The signal was then recorded on an oscilliscope.

It was found that there are basically four distinct types of wave shapes. The oscilliscope traces of these wave forms are shown in Figures 11-14. The centerline of all of the traces is at ground potential. Figure 15 shows where on the V-I curve the regions are located. In the T-form oscillation, it can be seen that there is an increase in the frequency with increase in current (Fig 16). Sabadil makes a similar observation in his paper.

In all our observations, the T-form waves ranged in frequency from 8-22 kHz. The frequencies of the transition and sinusoid waves were higher ranging from 20 to 100kHz.

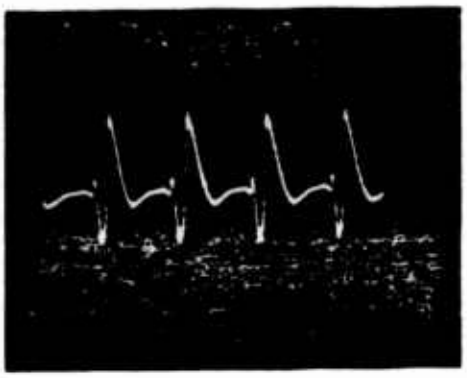

A=1.75volts
f=20kHz

Fig. 11:
T-Form

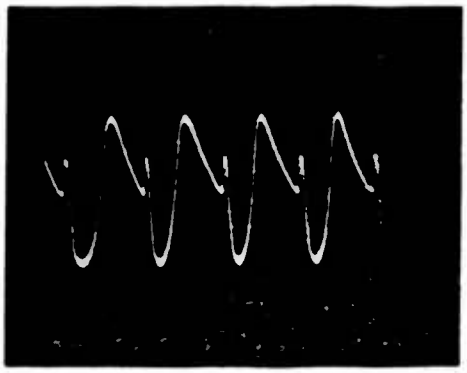

A=0.86volts
f=45kHz

Fig. 12:
Transition

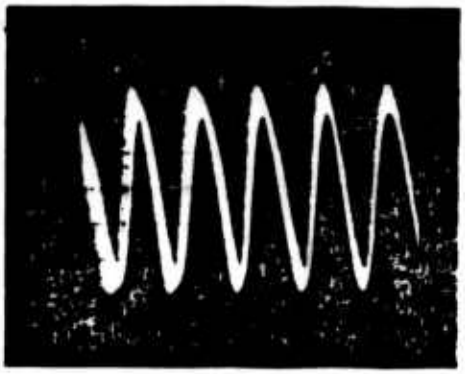

A=0.30volts
f=55kHz

Fig. 13:
Sinusoid

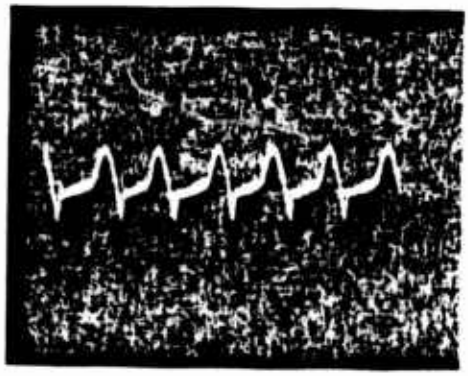

A=10.0mvolts
f=120Hz

Fig. 14:
H-Form

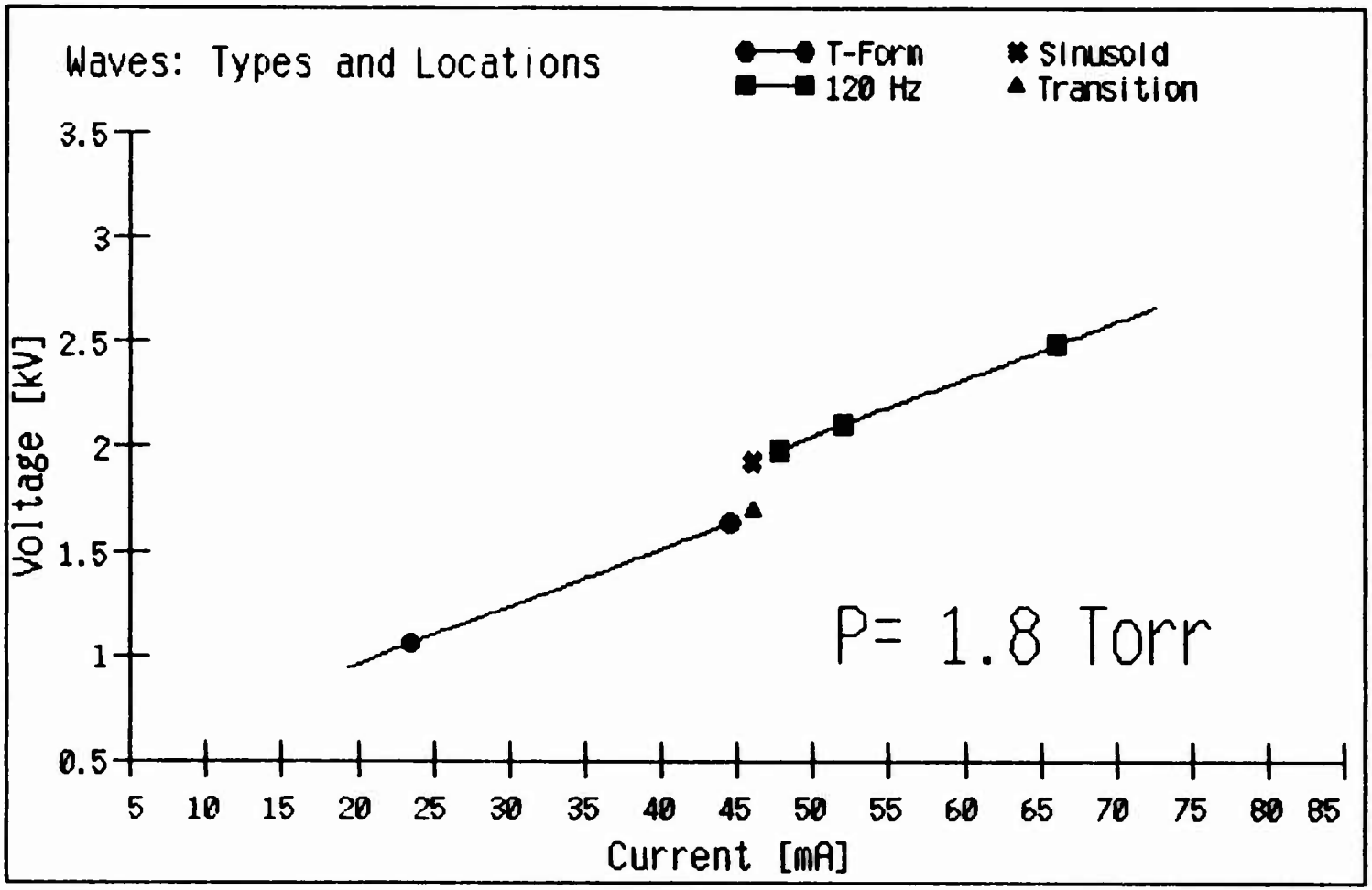

Fig 15. Location of Various Acoustic Forms

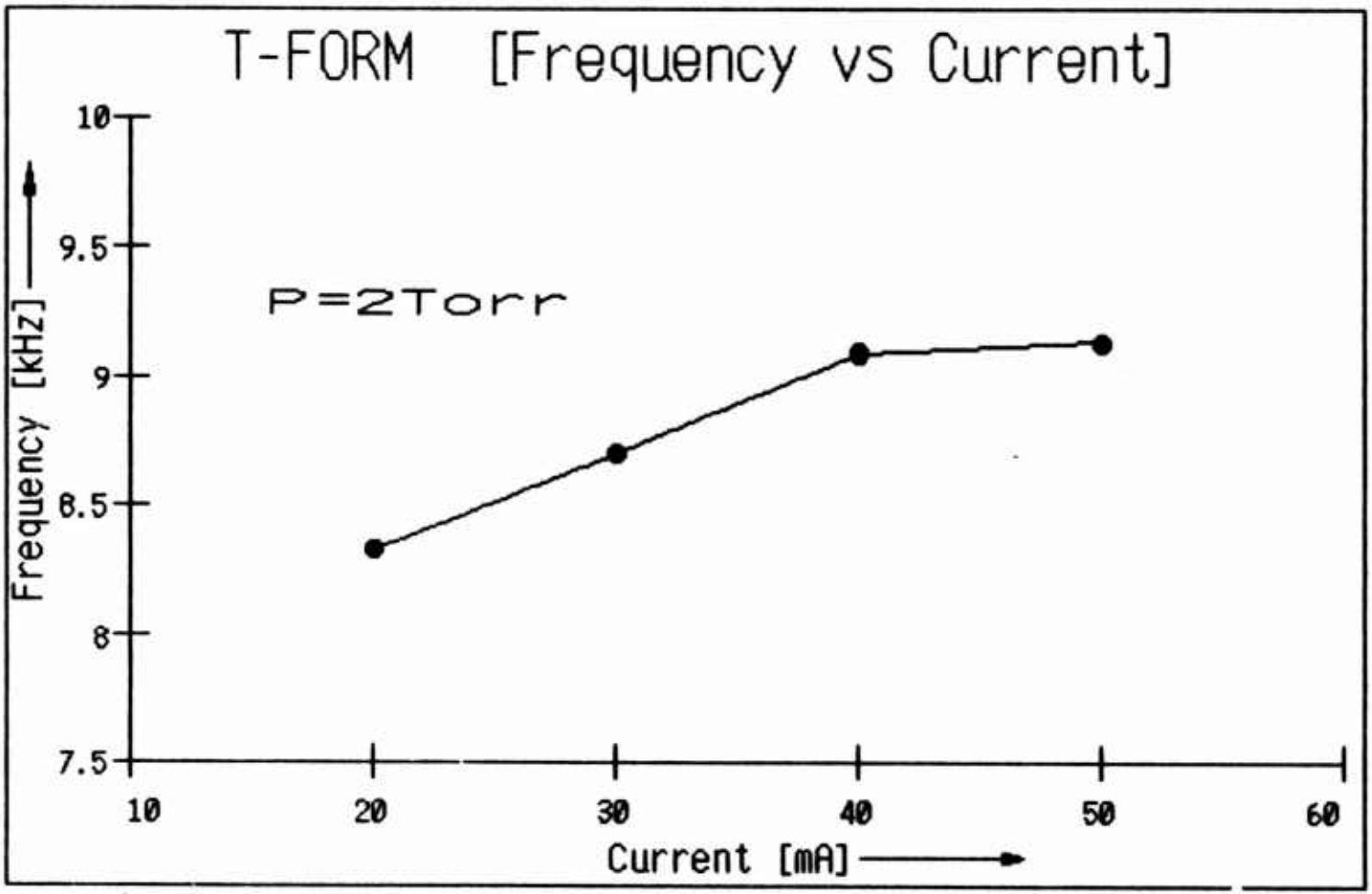

Fig 16. T-Form: Frequency vs. Current

Dettmer observed frequencies in his oxygen discharge from 20 to 90 kHz (9:65). According to Garscadden (15:66), ion acoustic waves can be found with frequencies ranging from 10^3-10^4 Hz. The 120 Hz signal seen in what should be the homogenous form of the discharge is further described by Garscadden as being circuit dependent. This H-Form ripple is higher than the 1 mV peak-peak ripple seen with the discharge tube short-circuited.

The determination of the type of oscillations involved can be done with a simple order of magnitude calculation. The electron and ion plasma frequencies are given respectively by

$$\omega_e = (4\pi n_e e^2/m_e)^{1/2} \tag{55}$$

and

$$\omega_i = (4\pi n_i Z^2 e^2/m_i)^{1/2} \tag{56}$$

where

Z = ionic charge
$n_{e,i}$ = number density of electron and ions
$m_{e,i}$ = mass of electrons and ions.

With the values for densities provided from Dettmer's dissertation we find that $\omega_e = 6*10^{10}$ s^{-1} and $\omega_i = 1*10^9$ s^{-1}.

The speed of an ion sound wave traveling in a plasma is given by

$$c_s \approx (ZT_e/m_i)^{1/2} \tag{57}$$

If a stable acoustic mode is to be set up in the cavitiy, the wave must oscillate with a frequency corresponding to the time it takes the wave to travel the length of the discharge and back again. This is given by

$$f_A = c_s/(2L) \tag{58}$$

where L is the length of the cavity. This provides an acoustic wave frequncy for our cavity of 7 kHz which is very near the frequency of the T-form oscillation observed in Figure 16.

Oscillations in the discharge will cause trouble in some of the proposed experiments. In the optogalvonic effect for example, a laser is pulsed through the cavity and a change in the discharge voltage is recorded through an RC circuit. Fluctuations in the tube voltage due to acoustic waves may severely hamper any effort to detect the laser-induced signal. If an effort is made to filter out the acoustic wave fluctuations, the frequencies of the waveform must be known.

The T-form and transition-form of the acoustic waves are not sinusoidal. A number of Fourier components add together to provide the wave shape seen. It would be very difficult to build a filter that could compensate for such wave shapes. The sinusoidal waveform, however, should be easily filtered. An effort was made, therefore, to describe the existence regions of this waveshape. This data is shown as

a plot (Figure 17) of the range of currents over which the sinusoid exists at various tube lengths at a typical pressure of 1.2 Torr. It should be remembered that the acoustic sinusoid exists near the transition region and therefore occurs at lower currents for lower pressures.

At currents higher than sinusoid stability, the discharge enters the homogenous region. Here we find the H-form oscillation. Because of its small amplitude compared to the sinusoid, it is difficult to determine if, after filtering the sinusoid, the H-form ripple will still exist. If such is the case, it would make more sense to operate in the homogenous form of the discharge and dispense with total filtering of the circuit. While this 5 mvolt ripple is not desirable, it should not thwart the experiment. According to Gangully (13), a laser induced optogalvanic signal for our discharge should be on the order of the ion acoustic wave magnitude. Thus, a signal of 100 mV should be clearly visible in the H-form's 5 mV ripple.

Yet another acoustic wave phenomena must be considered for a pulsed laser experiment. The strata moving in the discharge correspond to varying amounts of ions, neutrals and electrons. Sabadil reports (39) that the spacing of the strata moving within the discharge are three millimeters for a pressure of 0.5 Torr and current of 7 mA. The spacing of the acoustic strata diminishes with increasing pressure and decreasing current.

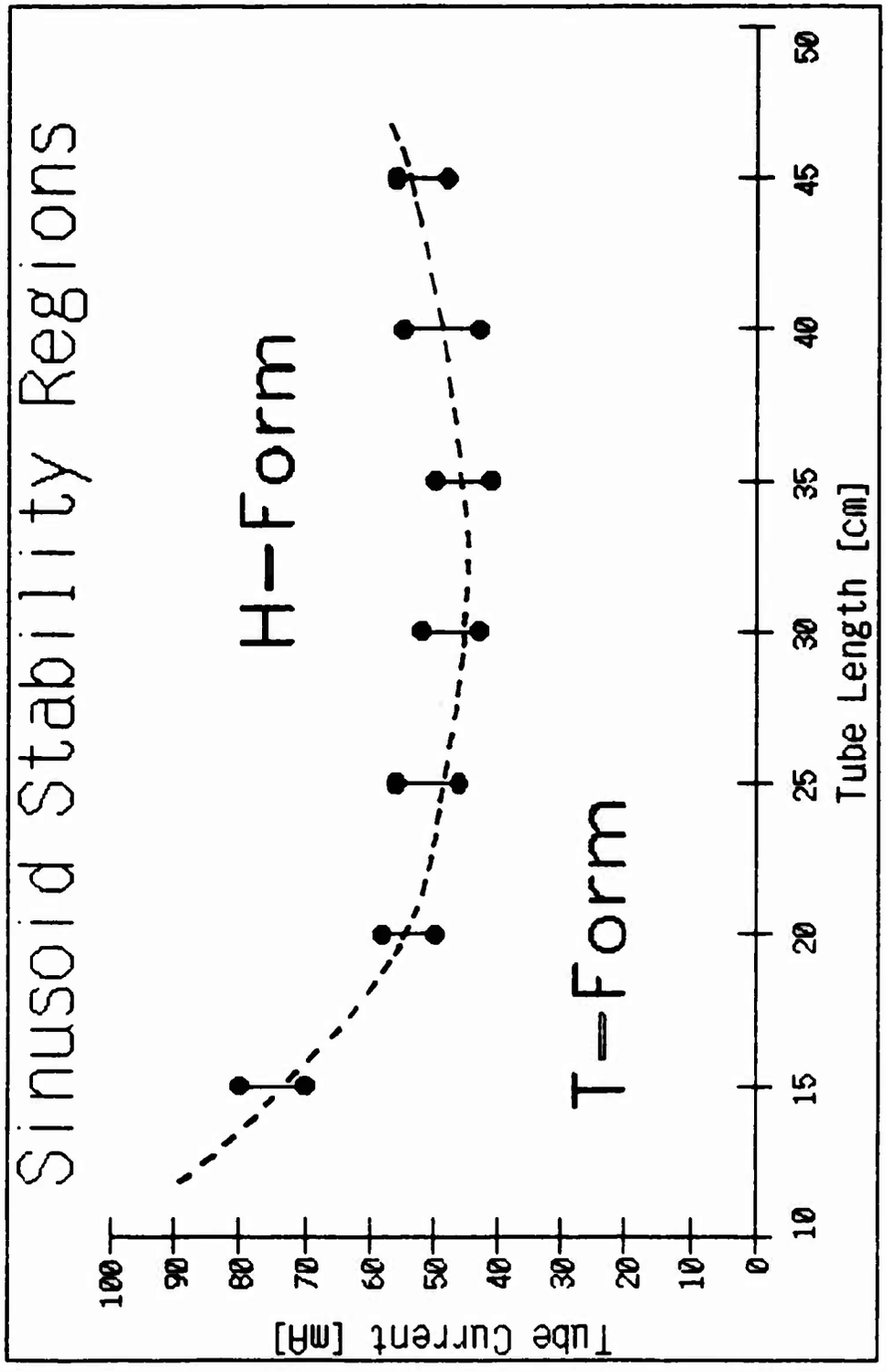

Fig 17. Existence of T-Form and H-Form on Either side of Sinusoid

If a pulsed laser experiment is performed in the sinusoid acoustic range, the spacing of the wave forms must be known. Typical laser pulses will be on the order of tens of nanoseconds. The pulse repetition rate must provide the proper averaging of the oscillating specie's densities. Signal aliasing will result if the pulse rate corresponds to a multiple of the oscillating frequency. The effects of aliasing will be reduced if the beam diameter is large enough to encompass a number of strata with a single pulse. Operation in the H-form of the discharge could reduce this problem further by eliminating the strong variation in species number densities.

V. Proposed Experimental Designs

We have shown that our discharge is typical of oxygen discharges observed in the past. It is reasonable to assume, therefore, that an experiment designed to determine the O^- density of this discharge would provide results applicable other discharge designs. Further, the ability of our discharge to adapt to a variety of experiments in a relatively short amount of time makes it extremely practical for all types of discharge experiments.

When work first began on this thesis, it was desired to determine the O^- density using fluorescent techniques. This would require tuning a dye laser to excite an electron in the ground state of O^- to a stable excited state. This state would decay back down to the ground state, after an appropriate lifetime, emitting fluoresced light. The intensity of this light would be proportional to the number density of the O^- ions.

According to Massey (30), in most cases stable excited states of atomic negative ions do not exist. From orbital extrapolation, Massey suggests (29) that there is no stable excited state for O^-. After extensive reasearch into the O- ion, no evidence of a stable excited state was found. According to Garscadden (14), no structure of such a state has been observed in photodetachment measurements. Bates and Massey (4) concluded that an excited state was not consistent with plausable values for the atomic

polarizability. Klein and Brueckner (25) suggest that no excited state should exist based on photo-absorption data. According to Hoffman (20), stable, singly excited states are not predicted for oxygen. Finally, Kutschera (26), concludes that there is no evidence of a doubly ionized oxygen ion (O^{2-}), which would have lent credibility to the existence of an excited state for O^-.

The only evidence for an excited state of an atomic negative ion in an electro-negative discharge is that reported by Popp (34) for an iodine discharge. He reports a line in the iodine spectrum at 585.3 nm.

Since the fluorescent method of determining the O^- density proved to be unsuccessful, other methods were investigated. We will present three such methods in this chapter. Each of these methods is based on the process of photodetachment of the negative oxygen ion O^-. Therefore, a background of the photodetachment process will be presented first. This will then be followed by the theoretical development of each individual experiment along with a description of the experiments' design.

The first of these experiments, absorption, proves to be the simplest fundamentally, but the least hopeful. The other two, variations of an optogalvanic experiment, are more complex, but previous experiments show the techniques to be promising.

Background

The photodetachment of the negative oxygen ion O^- is represented by

$$O^- + h\nu \rightarrow O + e^- \tag{59}$$

where $h\nu$ is a photon with an energy greater than the electron affinity of atomic oxygen (1.461eV). This corresponds to a wavelength ($\lambda=c/\nu$) shorter than 848.6 nm.

As light passes through the oxygen discharge, photons of energy greater than 1.461 eV will be absorbed in the photodetachment process. The intensity of the radiation passing through the discharge is then given by

$$\Phi(\lambda,x)=\Phi_o \exp\left[-\sigma(\lambda)\int n(x)dx\right] \tag{60}$$

where

Φ_o = Flux of incident radiation
$\sigma(\lambda)$ = photodetachment cross-section (cm^2)
$\eta(x)$ = $\int n(x)dx$ is the column density (cm^{-2})

It is easy to see that the greater the pathlength of the beam within the discharge, or the larger the photodetachment cross-section, the greater the number of incident photons will react with the negative ion. The greater the density of the O^- ions, the greater the number of photons that will react. Thus, if the the density of the O^- ion varies within the discharge (as we have shown it does in Chapter II), the

flux of a laser passing through the discharge should vary as the beam scans from the center outward. In all three of our experiments, it is desirable to have as much photodetachment as possible.

The photodetachment cross section is a function of the wavelength of the incident beam. Branscomb (5) has measured this cross-section and his results are reproduced in Figure 18. The cross-section is relatively constant at $6*10^{-18}$ cm^2 from 2.0eV to 3.5eV (620nm to 354nm). Lasers which emit in this region (which are numerous) are optimal for photodetachment experiments.

It should be remembered that there is another negative ion present in the oxygen discharge: O_2^-. The results of Dettmer (9:190), however, indicate that for operating conditions of interest the density of O^- is at least an order of magnitude higher than the density of O_2^-. Furthermore, Rees (35:38) shows the O^- photodetachment cross-section to be seven times larger than the cross-section of O_2^-.

Absorption

The most obvious application of the preceding discussion is absorption. A detailed explanation of the absorption process is given by Mitchell (31:92). If the flux of the light passing through the discharge varies as the beam scans from the center of the discharge to the tube walls, one can monitor this variation with some sort of photon detector.

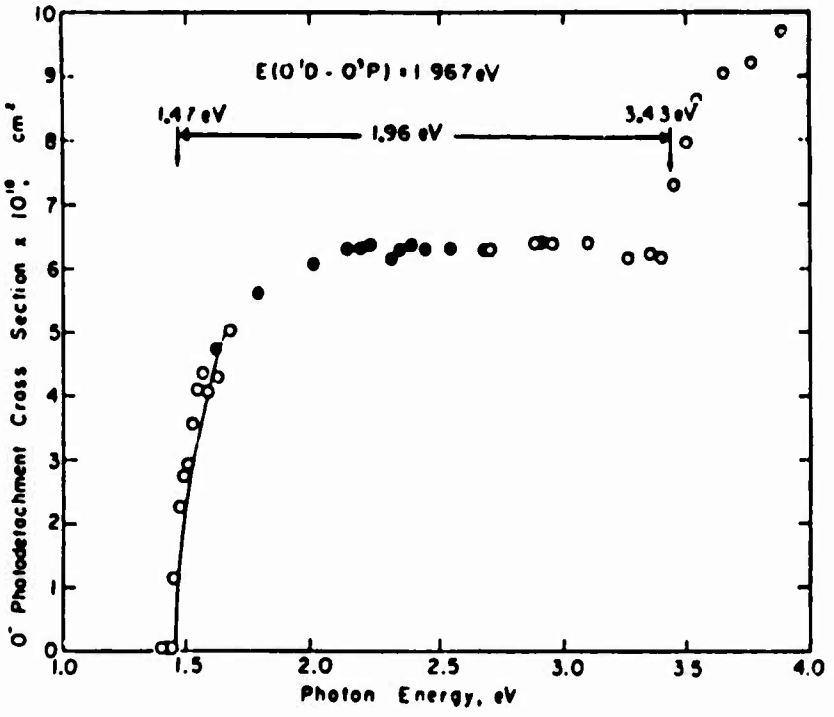

Fig 18. Photodetachment Cross-Section of O^-. (Branscomb:5)

With the discharge off, the density of O^- is zero. Thus, by Equation 60, the intensity of the light passing through the discharge is simply $\Phi(\lambda,x)=\Phi_o$. With Φ_o now known, the discharge is turned on and $\eta(x)$ is given by

$$\eta(x) = [1/\sigma(\lambda)]\ln(\Phi_o/\Phi) \qquad (61)$$

where, if we assume a constant ion density, $\eta(x)=n_-x$.

For a beam passing once through a discharge 5cm thick, and taking a typical value of $n_- = 10^{10}$ cm^{-3} from Dettmer (9:191), it's easy to show that $\Phi(\lambda,x) = .9999997*\Phi_o$. It is clear that such a small change in flux would be difficult to observe. We can, however, increase the path length x of the beam by making multiple passes through the discharge chamber. If, for example, two-hundred such passes are made, the path length increases to 1000cm. This gives a flux change $\Phi(\lambda,x) = .9994*\Phi_o$ which is significantly better.

During the course of our research, an attempt was made to observe the change in flux of a HeNe (632.8nm) laser passing though the discharge tube. Mirrors were placed on the outside of the cavity on either side of the discharge viewports. Two major difficulties were quickly discovered. First, the curved surfaces of the cylindrical discharge caused severe multiple reflections and refractions of the beam. Second, the fact that the mirrors were separate from the cavity, and the large vibrations in the room due to the pumps, caused both mirror and cavity to vibrate. These

vibrations caused the output signal to vary in a random manner (noise) and made it impossible to detect the small change in the signal required.

Time did not permit us to perform an experiment that would improve upon these conditions. Such an experiment, however, has been designed and will be presented here.

Figure 19 shows the general set-up of the experiment. The discharge itself is a slightly off-square glass tube. (Square glass discharges have been frowned upon in the past because of the instability of the glass under low pressures. No such instability exists in our experiment since the entire tube is enclosed in the vacuum chamber). The square sides of the tube provide for simple density measurement and prevent the smearing of the the beam seen in cylindrical discharges. The tube is slightly off-square to prevent multiple reflections from being confused with the original beam.

The plexiglass viewports used previously are now replaced with mirror-caps. The detailed design of the mirror-caps is shown in Appendix A. The mirror-caps allow the incident beam to pass through a porthole striking a mirror on the other side. Multiple reflections are thus created within the discharge. The beam finally exits the discharge through a porthole on the opposite mirror-cap. The interior mirrors are completely adjustable from the outside of the chamber allowing for a quick change in the number of passes desired. Since the mirrors now vibrate with the

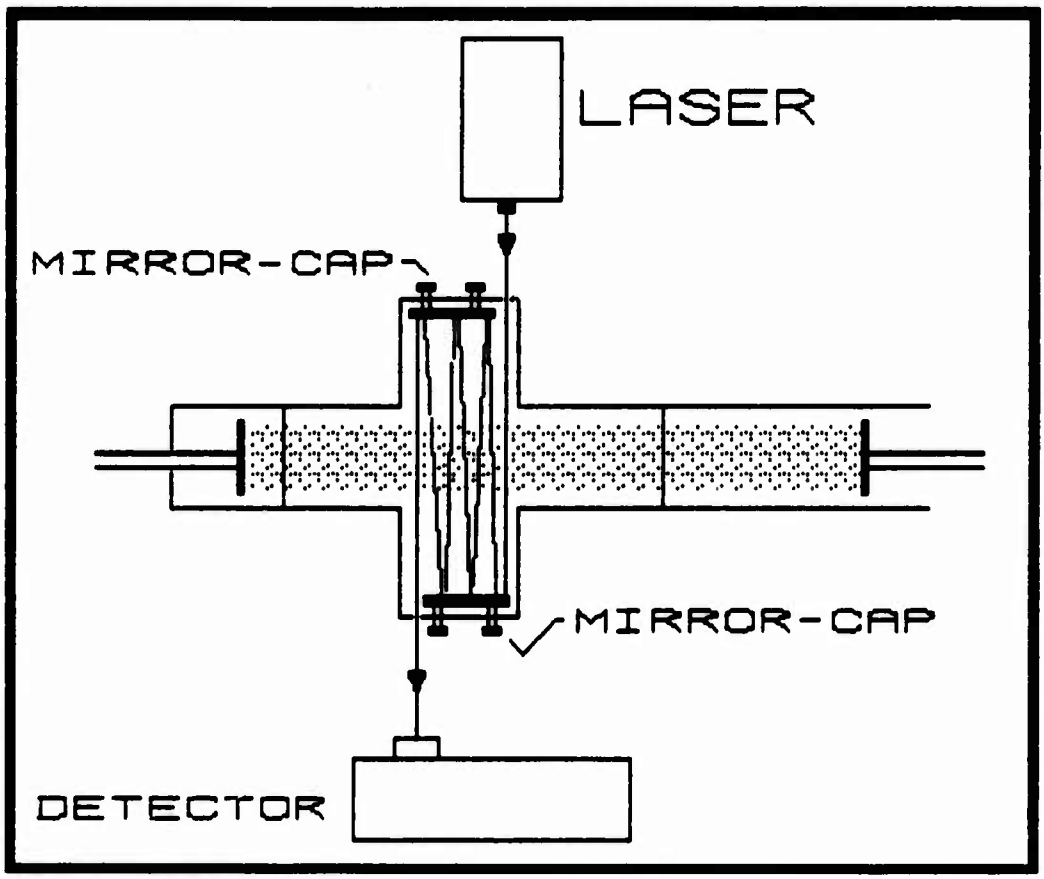

Fig 19. Absorption Experimental Design

gas discharge the intensity variation should be reduced considerably. This experiment should show if the O^- density can be determined via absorption. If a change in the signal is observed with the discharge on, then the interior square glass tube can be either raised or lowered to allow the density distribution to be scanned and compared to theory. In the event that the small change in the flux cannot be observed, we propose two optogalvanic experiments which hold some promise.

Laser Optogalvanic Effect

There are a number of articles describing the laser optogalvanic (LOG) effect (17, 18, 48). We will present here a discussion of the effect and how it can be applied to negative ion density measurements. We will then present an experiment using the optogalvanic effect.

In its purest form, the optogalvanic effect is a change in the electrical properties of a discharge caused by the illumination of the discharge with radiation having a wavelength corresponding to an atomic or molecular transition (16). If, for example, a laser excites atoms from a level with a small probability of ionization to a level wnich has a larger probability of ionization, the discharge current will increase and the discharge voltage will decrease. Using this technique, atomic concentrations as low as 10^8 cm^{-3} have been reported in experiments with uranium (24).

It is a natural extension to apply this method to photodetachment techniques. Thus, if a laser beam of sufficient energy passes through a discharge containing negative ions, the photodetachment process of Equation (59) will take place. There will then be an increase in the tube current and a corresponding decrease in the tube voltage. Such an experiment has already been performed to measure the photodetachment cross-section of the I^- ion (49).

A design of our proposed LOG experiment is presented in Figure 20. There are a number of variations to the experiment, but the fundamental principles remain the same. Since we are concerned only with the photodetachment of the negative ion, we need not concern ourselves with tunable lasers. Still we must operate in the region where the photodetachment cross-section is largest (620nm to 354nm).

The laser source can be either chopped CW or pulsed. Typically a CW laser output of hundreds of milliwatts (possibly argon-ion) can be chopped at around 1kHz and provide a signal of tens of millivolts for a 500-volt discharge (48:42). In the I^- photodetachment experiment of Webster (49), a pulsed dye laser was employed with energies of $\approx$400μJ/pulse and a pulse duration of $\approx$10ns. Haner (18) used a flashlamp-pumped dye laser and obtained a LOG signal with 4mJ/pulse with a .3μs pulse duration.

Typical LOG signal durations are of the order of tens of microseconds. The LOG signal obtained by Webster is shown in Figure 21. Here, a ten nanosecond pulse provided a

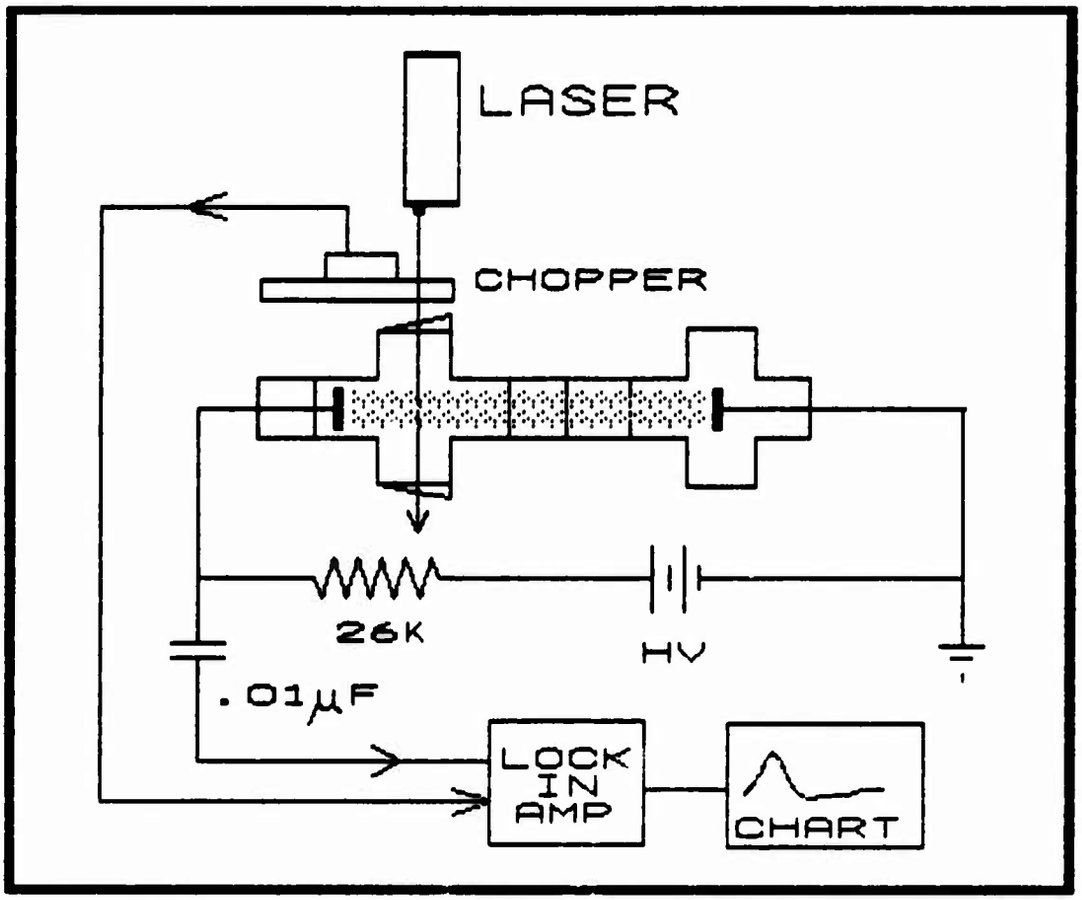

Fig 20. Optogalvanic Experimental Design

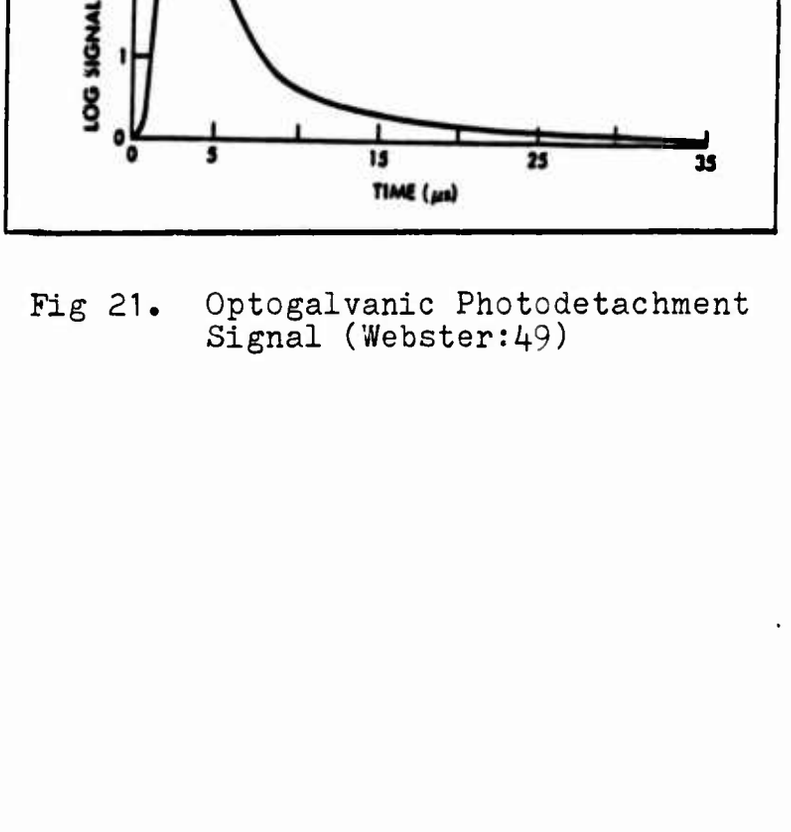

Fig 21. Optogalvanic Photodetachment Signal (Webster:49)

signal which reached its peak in five microseconds. The need for a short pulse duration is obvious.

The electronic circuitry shown in Figure 20 is typical of previous LOG experiments. Current-limiting ballast resistors from 1-100 kohms and coupling capacitors of .01μF with following low impedence detector circuits will allow response to signals with time constants less than a microsecond. The lock-in amplifier may be replaced with a simple boxcar averager or signal averager.

It is easy to see that there are a number of variations to a LOG experiment. The particular method employed depends on the equipment available at the time. We were unable to perform a LOG experiment since we did not have an appropriate laser source. An experiment was to be attempted with a low power nitrogen-pumped dye laser, but the laser was never approved for use.

Once the proper equipment is obtained, the experiment is straight forward. According to Bacal (3), the photodetachment fraction (the ratio of the number of negative ions ionized ($\Delta n-$) to the number of negative ions (n_-) is given by

$$\Delta n_-/n_- = 1 - \exp\{-[\mathcal{E}/A][\sigma/(h\nu)]\} \qquad (62)$$

where

$\mathcal{E}$ = Laser pulse energy
A = effective area of laser beam (πr^2)
σ = photodetachment cross-section
$h\nu$ = energy per photon.

Thus, at sufficiently high pulse energies total photodetachment occurs. Since the change in the LOG signal is proportional to the change in the electron density, and since for a photodetachment fraction near 100% the change in the electron density is equal to the number of negative ions, the LOG signal is proportional to the negative ion density.

The laser can now scan the discharge from the inside of the tube out to the walls while the LOG signal is monitored. The change in the LOG signal should correspond to a variation of negative ion density in the discharge tube.

Because oxygen is a strongly electro-negative gas, it is feared that once the free electrons are produced from photodetachment they will simply be swept up by the discharge. The principle loss of free electrons in the discharge is through dissociative attachment. Operating in the H-form of the discharge should help reduce the effects of dissociative attachment since the density of molecular oxygen is reduced. If, however, the LOG signal is too small to be detected, there is another method for determining the O^- density.

Probe LOG Signal

In order to prevent the electrons freed by photodetachment from being lost to the plasma, a method must be developed that will sweep up the electrons as soon as they are detached. Such a method involves placing a small

cylindrical probe into the discharge. The laser beam is then directed adjacent to and along the axis of the probe and the detached electrons are monitored by a change in probe current.

Joseph Taillet first performed such an experiment in 1969 in an effort to measure the negative ion density in an oxygen plasma (43). Taillet found that the increase in the observed electron density around the probe was ten times the initial electron density. He reported that the change in electron density was given by

$$\Delta n_e = \beta n_e \sigma \Sigma \Delta t \qquad (63)$$

where

β = the ratio of the negative ion to electron density
σ = the photodetachment cross-section of O^-, ($5*10^{18}$ cm^2) for the wavelength of a ruby laser.
Σ = flux (10^{24} photons s^{-1} cm^{-2})
Δt = pulse duration (60 nanoseconds)

This provided him with a value of $\beta \approx 30$.

In 1979, Bacal described more thouroughly an experiment for the determination of negative ion densities by photodetachment (2). The technique, used by one of her doctoral students, showed excellent agreement with negative ion densities found via mass spectroscopy (6). A modification of her experimental design as it applies to our discharge is presented in Figure 22. Here, a probe is inserted in the discharge, and the laser pulse is passed along its length. The free electrons produced by photodetachment are then

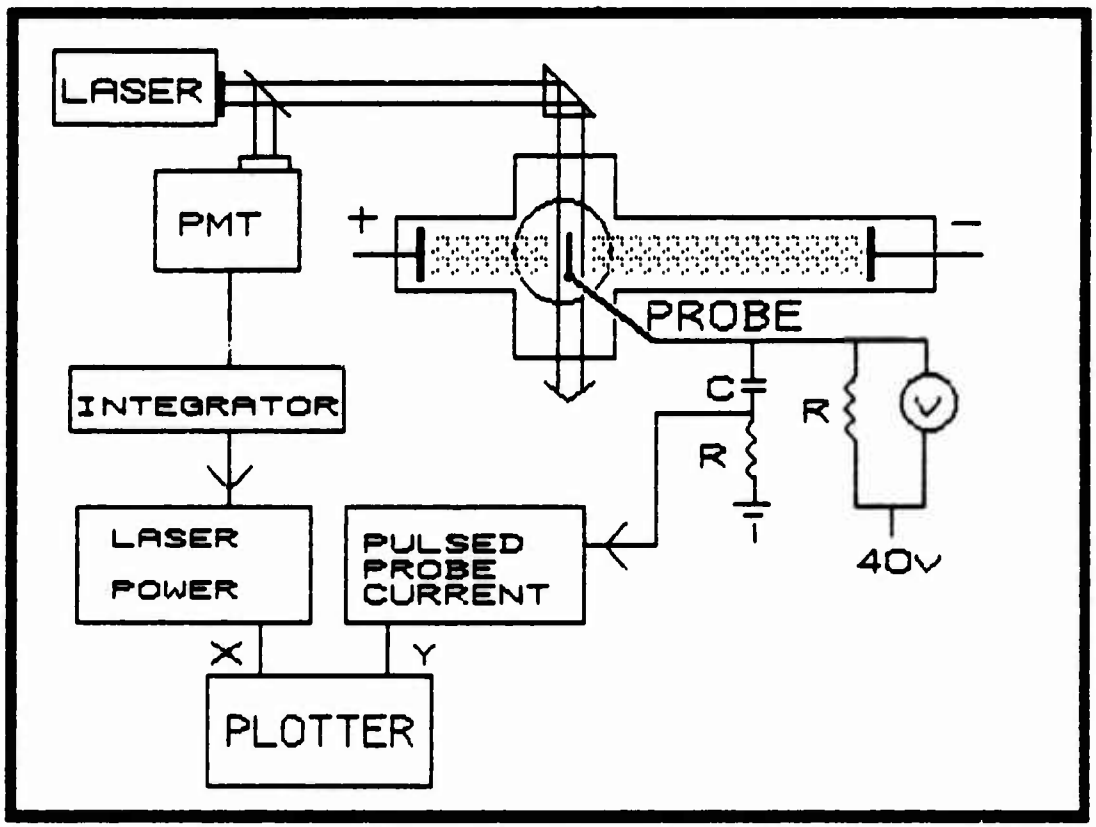

Fig 22. Probe LOG Experimental Design

swept up by the probe which is given a 10-50 volt bias. The sudden change in voltage is picked up by the capacitor and the resulting change in current can be recorded on a scope. As in the LOG experiment, if the laser is pulsed at a regular frequency, the signal may be averaged.

Bacal used a pulsed Ruby laser with a 30 ns pulse duration and 1 J/pulse energy delivery. Since the system was single pulse, the laser pulses were monitored by a PMT after the beam was split. The injected laser power can be monitored after it passes over the probe by a calorimeter placed within the vacuum chamber.

The best probe geometry is one in which the probe area inside the laser beam is larger than the probe area outside of the laser beam. Bacal used a self-supporting probe of diameter 0.5mm to measure relative ion densities and another probe with a radius less than 3 Debye lengths to measure absolute ion densities using Langmuir theory. This is done by using

$$n_-/n_e = \Delta n_e/n_e = \Delta j_{PROBE}/j_{PROBE\ DC} \qquad (64)$$

where

Δj = the change in probe current density
j = dc probe current density

when the photodetachment fraction is near 100%. Clearly if the electron current is then known, the ion density can be determined. It should be noted here that for

the typical operating conditions of our discharge the maximum Debye length $\{\lambda=[T_e/(4\pi ne^2)]^{1/2}\}$ is on the order of 0.05cm (9:5).

Bacal found no change in measurable signal when the probe was completely out of the laser beam. She found that only the portion of the probe immersed in the laser beam is effective for measuring the photodetachment current. This then provides the change in probe current densty Δj, while the entire probe area in the plasma provides the dc probe current density.

In Bacal's experiment, a dc current of 2.6 mA was obtained. The pulsed probe current had a rise of 0.4 μsecs and peaked at about 0.7 mA. The signal then decayed in 5.0 secs. For the purpose of ion diagnostics, only the peak of the signal need be considered to determine the density distribution.

In order to determine the distribution of the negative ions, both probe and beam must be moved together from the center of the chamber to the chamber walls. It may also be feasible to maintain a constant beam-probe relationship and instead move the interior chamber. The resulting variation in peak probe signal will correspond to the ion distribution and can then be compared to theory.

VI. Discussion and Conclusions

The objective of this thesis was to develop a firm foundation, both theoretically and experimentally, upon which a follow-up experiment could be performed. Our ultimate goal, of course, is to obtain experimental data concerning the radial distribution of the negative oxygen ion (O^-) in the positive column of a pure oxygen discharge.

We have developed an experimental chamber that can be easily adapted to a variety of discharge designs. In particular, it allows the use of a square discharge tube. Thus, refractions and multiple laser reflections are reduced. All three of the experiments presented in this thesis may be performed with minimal modification of the chamber design.

A theoretical model was presented to determine the density distribution of the oxygen negative ion in a square discharge. This model is based on Lee's theory, considered by Clouse to be the most consistent. It was observed that the density varies as the cosine from the center of the discharge to the walls. A plot of the density variation as seen by a laser scanning such a square discharge is also presented (Fig 5).

Various operating characteristics of the discharge were also investigated. The major impurities observed in the discharge were hydrogen and carbon monoxide. It is believed that the hydrogen was due to water vapor while the carbon

monoxide is a product of the new discharge glass. The observed spectral lines also showed that most visible lasers can be used for photodetachment experiments.

Voltage and current plots showed the transition regions for our discharge as functions of pressure. It is believed that the high field form of the discharge is dominated by direct molecular ionization processes. This high field form behaves much like a two-component plasma since electron densities are greater than negative ion densities. Transition to the low field form is characterized by the domination of negative ion densities over electron densities and the fact that attachment/detachment processes take control over ionization. The reduced field oscillates between these processes to sustain itself, thus creating accoustic waves.

It was observed that in the transition region near the high field form of the discharge the acoustic waves became nearly sinusoidal. At currents higher than the transition the H-form is nearly homogenous (without strata). Only a 5 mV, 120Hz ripple exists.

Three experiments were presented to determine the radial density distribution of the negative ion. The three experiments involve absorption and two variations of the optogalvanic effect. It was shown that all depend on the photodetachment process. Fortunately, the photodetachment cross-section is much higher for O^- than it is for the next most dense negative ion O_2^-.

In order to perform each of these experiments it is necessary to know in which acoustic regime the discharge is operated. It is expected that when the square discharge is implemented, the acoustic wave phenomena will change. An understanding of the types of waves in the discharge is imperative so that the proper beam width and chopping frequency are used.

The most needed improvements in the design of the discharge include the use of a floating table and a method for cooling the cathode side of the discharge. This should provide more accurate results as well as allow the discharge to be operated for longer periods of time.

It is believed that the design of the the main discharge chamber and the theoretical development of the square discharge are presented here for the first time. The operation of an oxygen discharge, however, has been a topic of discussion for decades. None of the phenomena observed over the course of our work was inexplicable. Most of what was seen has been reported in the past. With this in mind, it should seem reasonable that the discharge design could be used for a variety of discharge experiments.

Appendix A

Mirror Design for Absorption Experiment

We present here the design of the mirrors to create multiple passes through the discharge. Each mirror is mounted on a flange that is mounted to the ports of one of the crosses on the main chamber (see Figure A-1). The mirror design is modeled after the NRC model MM-2A mirror movement. (Newport Research Company, Fountain Valley, CA.)

The screws that provide the side to side variation are placed in the flange described above (Figure A-2). In order to maintain a vacuum, O-rings surround the screws. The design is similar to that of the adjustable electrodes.

Two springs hold the mirror support (a metal plate as seen in Figure A-3) against the adjustment screws. Laser light can enter the chamber through a glass porthole on either side of the mirror plate, and exits in like manner after the desired number of passes on the other side.

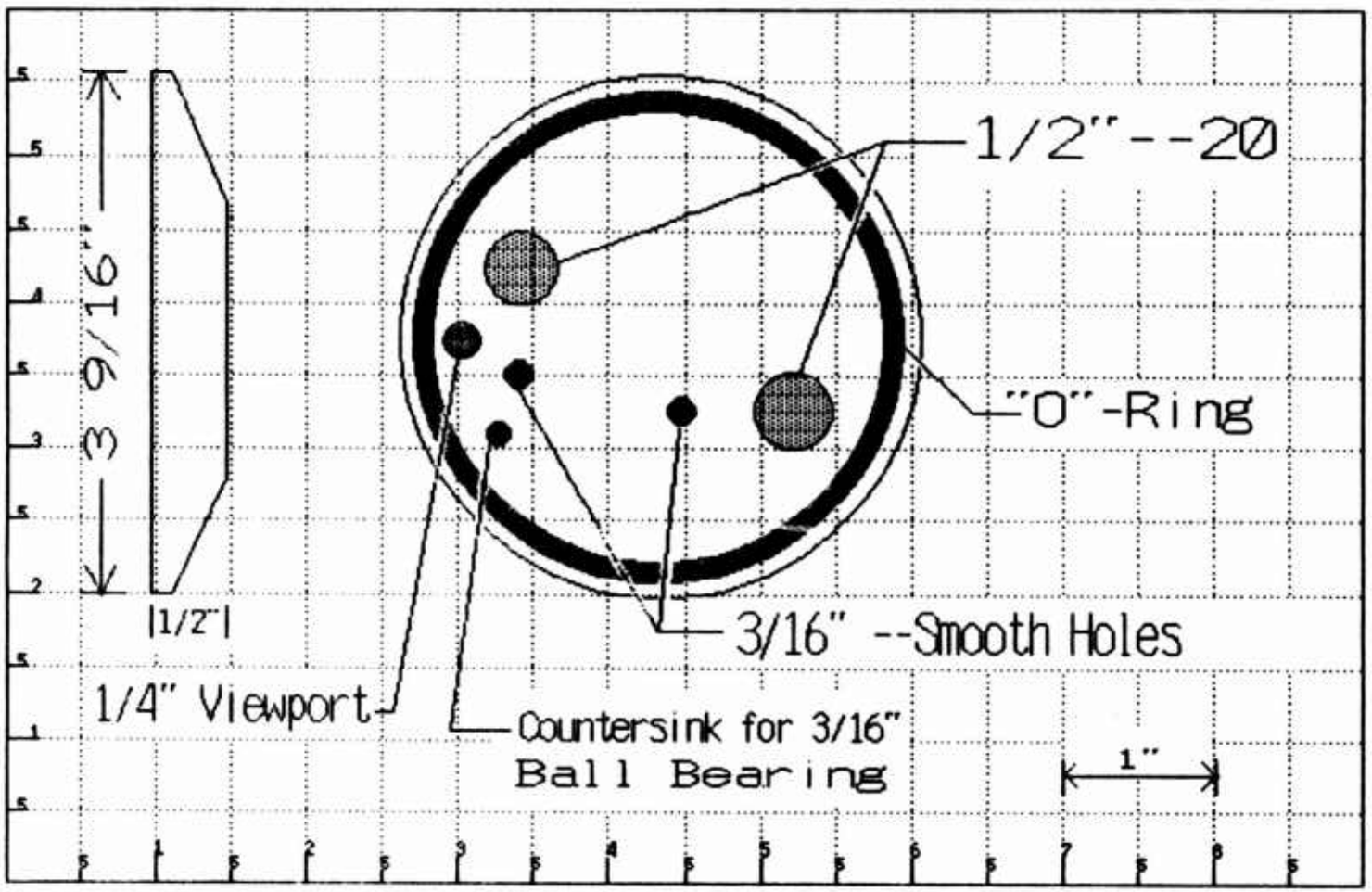

Fig A-1. Mirror Flange Design (Outside Cap)

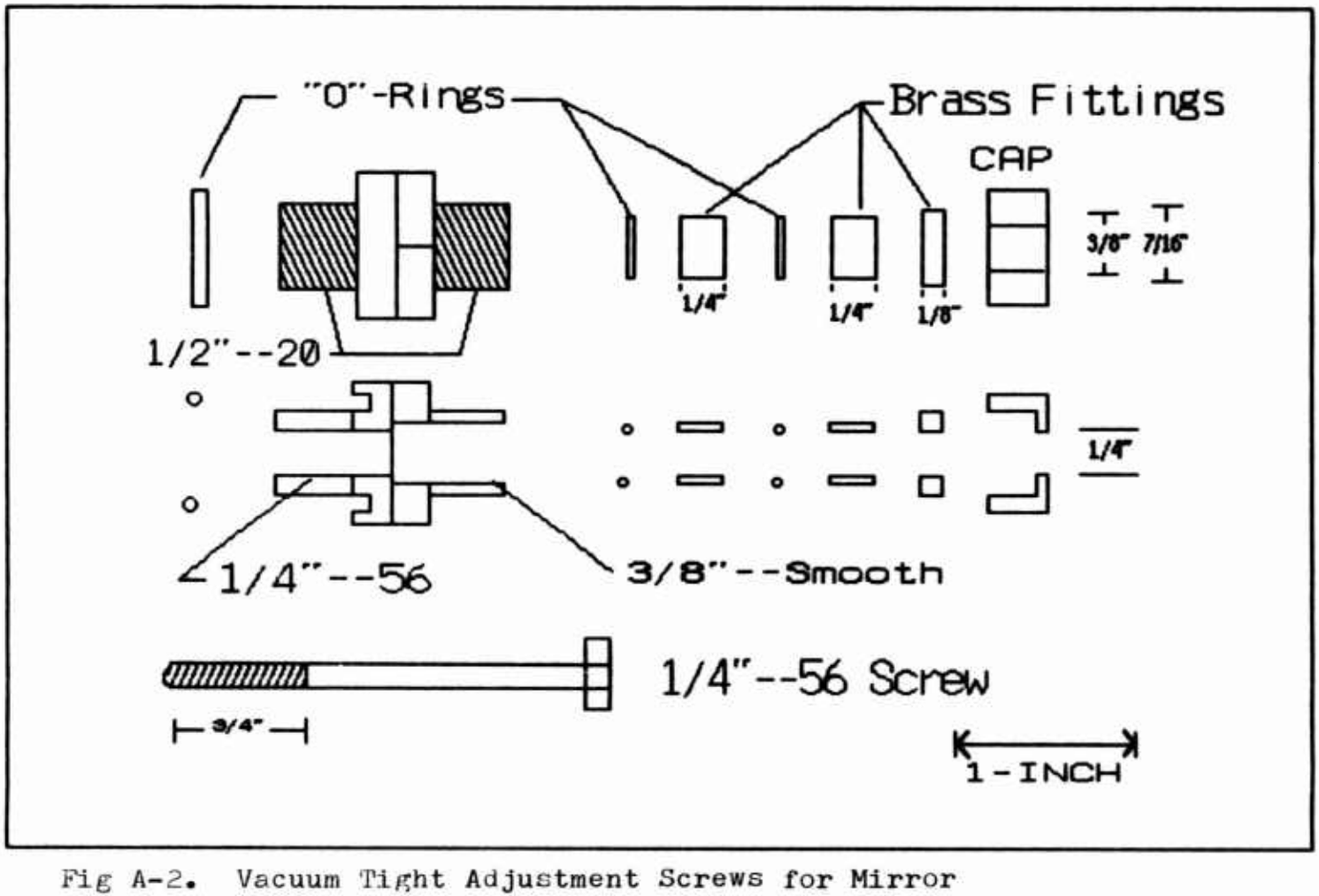

Fig A-2. Vacuum Tight Adjustment Screws for Mirror

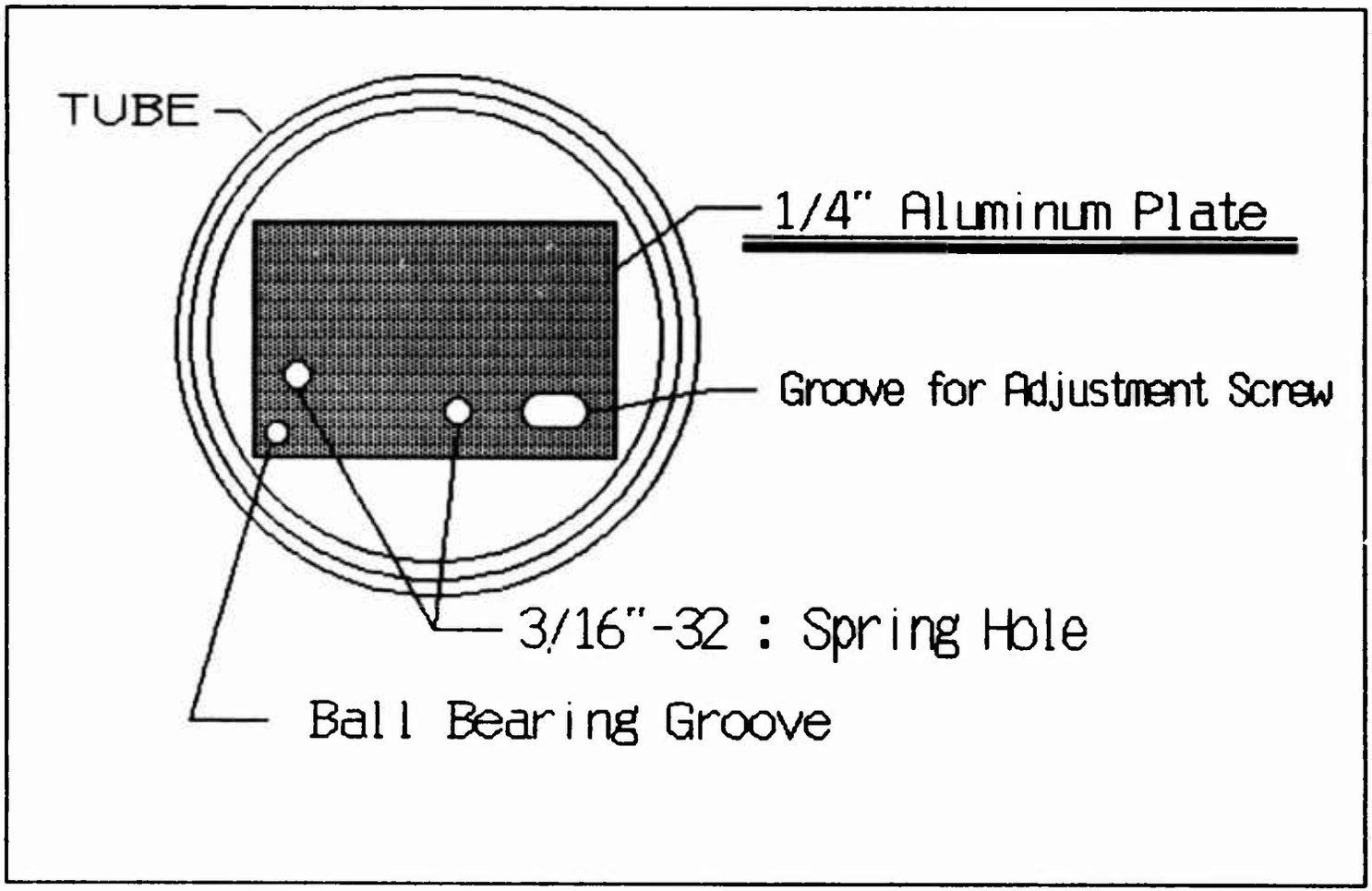

Fig A-3. Inside Mirror Plate for Absorption Experiment

Bibliography

1. Bacal, M. and H.J. Doucet. "Generation of Ion-Rich Plasma in Electro-Negative Gases (Oxygen)," Vacuum, 24: 595-600 (1974)

2. Bacal, M. and others. "Measurement of H^- density in plasma by photodetachment," Review of Scientific Instruments, 50: 719-720 (June 1979)

3. Bacal M. and G.W. Hamilton. "H^- and D^- Production in Plasmas," Physical Review Letters, 42: 1538-1540 (June 1979).

4. Bates D.R. and H.S.W. Massey "The Basic Reactions in the Upper Atmosphere," Proceedings of the Royal Society (London), A192: 1-16 (23 Decmber 1947)

5. Branscomb, L.M. and others. "Oxygen Metastable Atom Production Through Photodetachment," Journal of Chemical Physics, 43: 2906-2907 (September 1965)

6. Bruneteau Mordin, A. Etude Sur l'Ion Negatif d'Hydrogene dans des Descharges a Basse Pression. PhD dissertation. University de Paris, Sciences Physiques, 5 July 1983.

7. Chapman, B. Glow Discharge Processes. New York: John Wiley and Sons, 1980.

8. Clouse, 2nd Lt C.J. Schottky Theory of Three Component Plasmas. MS thesis. School of Engineering, Air Force Institute of Technology (AU), Wright-Patterson AFB, OH, January 1985.

9. Dettmer, Col J.W. Discharge Processes in the Oxygen Plasma. PhD dissertation. School of Engineering, Air Force Institute of Technology (AU), Wright-Patterson AFB OH, December 1978 (AD-AO-66196).

10. Edgley, P.D. and A. von Engel. "Theory of Positive Columns in Electronegative Gases," Proceeding of the Royal Society (London), A370: 375-387 (1980)

11. Fehsenfeld, F.C. and others. "Laboratory Measurements of Negative Ion Reactions of Atmospheric Interest," Planetary Space Science, 15: 373-379 (1967)

12. Franklin, R.N. Plasma Phenomena in Gas Discharges. Oxford: Oxford University Press, 1976.

13. Gangully, B. Research Physicist. Personal Interview. Advanced Plasma Research Group, Aero Propulsion Lab, Wright-Patterson AFB OH, August 1986

14. Garacadden, A. Research Pysicist. Personal interview. Advanced Plasma Research Group, Aero Propulsion Lab, Wright-Patterson AFB OH, June 1986.

15. -----. "Ionization Waves in Glow Discharges," Gaseous Electronics, edited by Merle N. Hirsh. New York: Academic Press, 1978.

16. Goldsmith, J.E.M. and J.E. Lawler. "Optogalvanic Spectroscopy," Contemporary Physics, 22: 235-248 (1981)

17. Green, R. B. and others. "Galvanic Detection of Optical Absorptions in a Gas Discharge," Applied Physics Letters, 29: 727-729 (December 1976)

18. Haner, D.A. "Time Resolved Study of the Laser Optogalvanic Effect in I_2," Chemical Physics Letters, 96: 302-306 (April 1983)

19. Herzberg, G. Molecular Spectra and Molecular Structure (Second Edition). New York: Van Nostrand Reihnhold Company, 1950.

20. Hoffman H. "O^--ion Radiation in the Spectrum of an Oxygen Arc Plasma," Journal of Quantitative Spectroscopy and Radiative Transfer, 21: 163-179 (1979)

21. Howatson, A.M. An Introduction to Gas Discharges (Second Edition). Oxford: Pergamon Press, 1965.

22. Ingold, J. "Schottky Theory of the Positive Column with Electron Attachment," 33rd Gaseous Electronics Conference, (1980).

23. -----. "Glow Discharges at DC and Low Frequencies," Gaseous Electronics, edited by Merle N. Hirsh. New York: Academic Press, 1978.

24. Keller, R.A. and others . "Optogalvonic Detection in Uranium Hollow-Cathode Discharge," Journal of the Optical Society of America, 69: 738-742 (May 1979)

25. Klein, M.M. and K.A. Brueckner. Physical Review, 111: 1115 (1958)

26. Kutschera, W. and others. "A search for Doubly-Charged Negative Ions Via Accelerator Mass Spectrometry," Argonne National Laboratory Government Report. DE83-014321 (December 1983)

27. Lee, D.A. and F.D. Lewis "Multiple Equilibria in the Oxygen Positive Column," Journal of Applied Physics, 51: 4699-4705 (September 1980).

28. Lewis, Capt F.D. Radial Structure in the Low Pressure Equilibrium Oxygen Discharge. MS thesis. School of Engineering, Air Force Institute of Technology (AU), Wright-Patterson AFB OH, December 1978.

29. Massey, H.S.W. Negative Ions (Third Edition). Cambridge: Cambridge University Press, 1976.

30. -----. Negative Ions (Second Edition). Cambridge: Cambridge University Press, 1950.

31. Mitchell, A.C.G. and M.W. Zemansky. Resonance Radiation and Excited Atoms,. London: Cambridge University Press, 1934.

32. Pearse, R.W.B. and A.G. Gaydon. The Identification of Molecular Spectra (Third Edition). New York: John Wiley and Sons, 1963.

33. Penkin, N.P. and others. "Investigation of the Electrokinetic Properties and of the Dissociation of O_2 Molecules in an Oxygen Discharge," Soviet Physics and Technical Physics, 27: 945-949 (August 1982)

34. Popp, H.P. "Spectroscopy of Negative Ion Radiation Emitted from a Low Current Arc," Vacuum, 24: 551-555 (1974).

35. Rees, J.A. "Fundamental Processes in the Electrical Breakdown of Gases," Electrical Breakdown of Gases, edited by J.M. Meek. New York: John Wiley and Sons, (1978)

36. Rundle, H.W. and others. "Chemical Reactions in Electric Discharges," Canadian Journal of Chemistry, 44: 2995-3007 (1966)

37. Sabadil, H. "On the Radial Structure of the Diffusion Designated Positive Column of the Oxygen Discharge at Low-Gas Pressure," Beitrage Aus Der Plasma Physic, 13: 235-251, 1973. (FTD-HC-23-2824-74)

38. -----. "On the Mechanism of the Homogeneous Positive Column in Oxygen Low-Pressure Discharge," Beitrage Aus Der Plasma Physik, 11: 58-66, 1971. (FTD-HC-23-1387-74)

39. -----. "Stratification Phenomena in the Positive Column of a Low Pressure Oxygen Discharge," Beitrage Aus Der Plasma Physik, 6: 305-317, 1966. (FTD-HC-23-1385-74)

40. Schottky, W. Phys. Z, 25: 635 (1924)

41. Schultz, G.J. "Studies in Electron Collisional Processes in Atmospheric Gases," Yale University, New Haven, Conn. Research and Technology Work Unit Summary, DAOB9229. (30 Oct 1974)

42. Shampine, L.F. and M.K. Gordon. Computer Solution of Ordinary Differential Equations. San Fransisco: W.H. Freeman and Company, 1975.

43. Taillet, Joseph, "Determination des Concentrations en Ions Negatifs par Photdetachement-Eclair," Comptes Rendus Academie de Science (Paris), B269: 52-54 (1969)

44. Thompson, J.B. "The ion balance of the Oxygen D.C. Glow Discharge," Proceedings of the Royal Society (London), A262: 519-528 (1961)

45. -----. "Negative Ions in the Positive Column of the Oxygen Discharge," Proc. Royal Society, 73: 818-821 (1959)

46. Von Engel, A. Ionized Gases (Second Edition), Oxford: Clarendon Press, 1965.

47. Weast, R.C. CRC Handbook of Chemistry and Physics (66th Edition), Boca Raton FL: CRC Press Inc. (1986)

48. Webster, C.R. and C.T. Rettner. "Laser Optogalvanic Spectroscopy of Molecules," Laser Focus, 19: 41-46+ (February 1983)

49. Webster, C.R. and I.S. McDerrmid. "Laser Optogalvanic Photodetachment Spectroscopy: A New Technique for Studying Thresholds with Application to I^-," Journal of Chemical Physics, 78: 646-651 (January 1983).

Vita

J. Mark DelGrande was born [redacted] In 1980, he graduated valedictorian from [redacted] Subsequently, he attended Oregon State University, from which he graduated in 1985, with high scholarship, given a Bachelor of Science degree in engineering physics.

After receiving his commission in the United States Air Force on 22 March 1985, he was assigned, direct accession, to the Air Force Institute of Technology to pursue an advanced degree in engineering physics.

UNCLASSIFIED

SECURITY CLASSIFICATION OF THIS PAGE

AD-A179 212

REPORT DOCUMENTATION PAGE

1a. REPORT SECURITY CLASSIFICATION: UNCLASSIFIED	1b. RESTRICTIVE MARKINGS
2a. SECURITY CLASSIFICATION AUTHORITY	3. DISTRIBUTION/AVAILABILITY OF REPORT: Approved for public release; distribution unlimited
2b. DECLASSIFICATION/DOWNGRADING SCHEDULE	
4. PERFORMING ORGANIZATION REPORT NUMBER(S): AFIT/GEP/ENP/86D-3	5. MONITORING ORGANIZATION REPORT NUMBER(S)
6a. NAME OF PERFORMING ORGANIZATION: School of Engineering; 6b. OFFICE SYMBOL (If applicable): AFIT/ENP	7a. NAME OF MONITORING ORGANIZATION
6c. ADDRESS (City, State and ZIP Code): Air Force Institute of Technology, Wright-Patterson AFB, Ohio 45433	7b. ADDRESS (City, State and ZIP Code)
8a. NAME OF FUNDING/SPONSORING ORGANIZATION; 8b. OFFICE SYMBOL (If applicable)	9. PROCUREMENT INSTRUMENT IDENTIFICATION NUMBER
8c. ADDRESS (City, State and ZIP Code)	10. SOURCE OF FUNDING NOS. — PROGRAM ELEMENT NO. / PROJECT NO. / TASK NO. / WORK UNIT NO.
11. TITLE (Include Security Classification): See Box 19	

12. PERSONAL AUTHOR(S): J. Mark DelGrande, B.S., 2nd Lt, USAF

13a. TYPE OF REPORT	13b. TIME COVERED	14. DATE OF REPORT (Yr., Mo., Day)	15. PAGE COUNT
M.S. Thesis	FROM _____ TO _____	1986 December	83

16. SUPPLEMENTARY NOTATION

17. COSATI CODES			18. SUBJECT TERMS (Continue on reverse if necessary and identify by block number)
FIELD	GROUP	SUB. GR.	Negative Ions, Ion Density Glow Discharges, Gas Discharges Oxygen Discharges, Plasma Diagnostics
20	09		

19. ABSTRACT (Continue on reverse if necessary and identify by block number)

Title: RADIAL DENSITY DISTIBUTION OF NEGATIVE ATOMIC OXYGEN IN THE OXYGEN POSITIVE COLUMN: AN EXPERIMENT

Thesis Chairman: Howard E. Evans, Lt Col, USAF
Instructor of Physics

Approved for public release: IAW AFR 190-1.
LYNN E. WOLAVER 5 March 87
Dean for Research and Professional Development
Air Force Institute of Technology (AFIT)
Wright-Patterson AFB OH 45433

20. DISTRIBUTION/AVAILABILITY OF ABSTRACT	21. ABSTRACT SECURITY CLASSIFICATION
UNCLASSIFIED/UNLIMITED ☒ SAME AS RPT. ☐ DTIC USERS ☐	UNCLASSIFIED

22a. NAME OF RESPONSIBLE INDIVIDUAL	22b. TELEPHONE NUMBER (Include Area Code)	22c. OFFICE SYMBOL
Howard E. Evans, Lt Col, USAF	513-255-5187	AFIT/ENP

DD FORM 1473, 83 APR — EDITION OF 1 JAN 73 IS OBSOLETE.

UNCLASSIFIED

SECURITY CLASSIFICATION OF THIS PAGE

This thesis develops the foundation for an experiment to determine the radial distribution of the negative atomic oxygen ion in the positive column of a plasma discharge. Lee's theory is modified to apply to a discharge of square cross-section. A new design for a discharge tube is presented. The operating characteristics of this tube are investigated: current-voltage measurements are made showing operating regimes of the T-form and H-form of the discharge, and acoustic waves are shown to exist in the T-region. Three experimental designs are presented to determine the radial density of the negative atomic oxygen ion, each involving photodetachment.